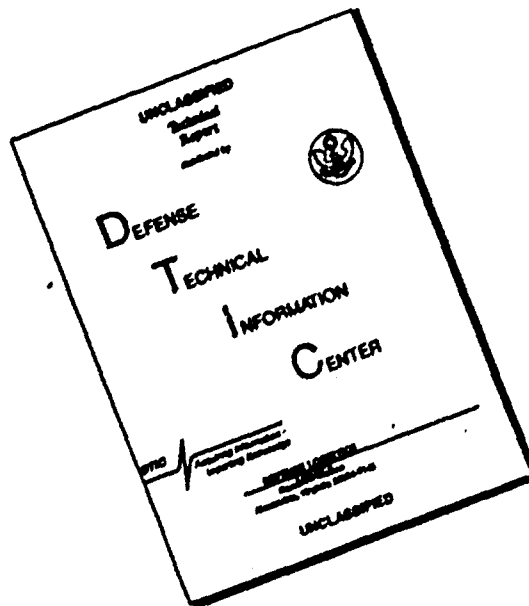


DISCLAIMER NOTICE



THIS DOCUMENT IS BEST QUALITY AVAILABLE. THE COPY FURNISHED TO DTIC CONTAINED A SIGNIFICANT NUMBER OF PAGES WHICH DO NOT REPRODUCE LEGIBLY.

AD A039801

CONTRACT REPORT S-78-17

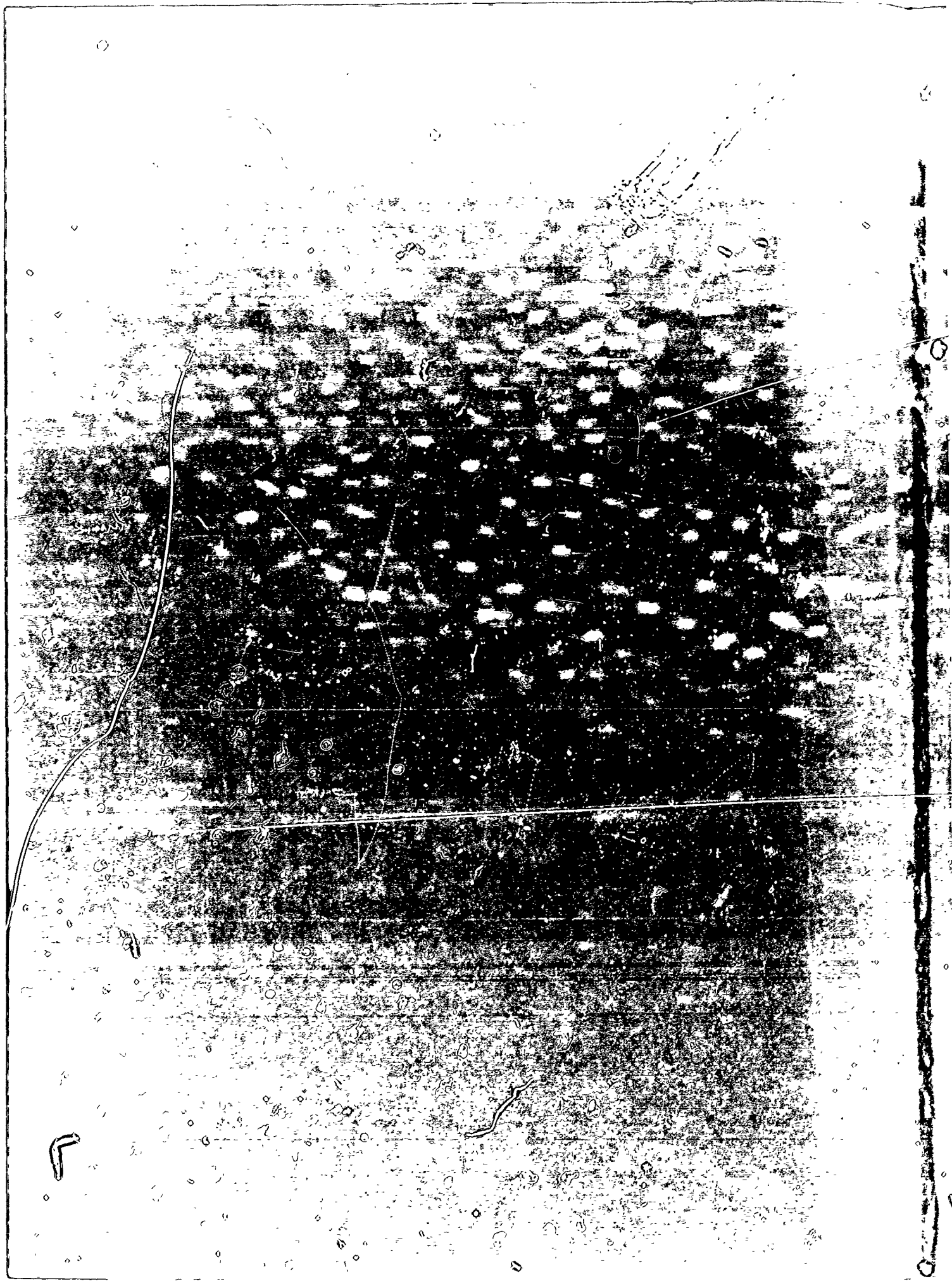
PORE PRESSURES IN SOFT GROUND UNDER SURFACE LOADING. INTERPRETATION OF FIELD RECORDS

R. H. B. M. P. M.
Chief, of Contract Group

September 1976

Field Report

Report for Public Affairs Information Bureau



Unclassified

SECURITY CLASSIFICATION OF THIS PAGE (When Data Entered)

| REPORT DOCUMENTATION PAGE | | READ INSTRUCTIONS BEFORE COMPLETING FORM |
|---|-----------------------|---|
| 1. REPORT NUMBER Contract Report S-76-10 | 2. GOVT ACCESSION NO. | 3. RECIPIENT'S CATALOG NUMBER |
| 4. TITLE (and Subtitle) PORE PRESSURES IN SOFT GROUND UNDER SURFACE LOADING; INTERPRETATION OF FIELD RECORDS. | | 5. DATE OF REPORT & PERIOD COVERED Final report, Jan 75 - Jul 76 |
| 6. AUTHOR R. H. G. Parry C. P. Wroth | | 7. PERFORMING ORG. REPORT NUMBER |
| 8. PERFORMING ORGANIZATION NAME AND ADDRESS University of Cambridge, England | | 9. CONTRACT OR GRANT NUMBER(s) |
| 10. CONTROLLING OFFICE NAME AND ADDRESS Office, Chief of Engineers, U. S. Army Washington, D. C. 20314 | | 11. PROGRAM ELEMENT PROJECT TASK AREA & WORK UNIT NUMBERS CWIS-31189 |
| 12. MONITORING AGENCY NAME & ADDRESS (if different from Controlling Office) U. S. Army Engineer Waterways Experiment Station Soils and Pavements Laboratory P. O. Box 631, Vicksburg, Miss. 39180 | | 13. REPORT DATE September 1976 |
| | | 14. NUMBER OF PAGES 37 |
| | | 15. SECURITY CLASS. (of this report) Unclassified |
| 16. DISTRIBUTION STATEMENT (of this Report) Approved for public release; distribution unlimited. | | 17. SECURITY CLASS. (of this report) Unclassified |
| 18. DISTRIBUTION STATEMENT (of the abstract entered in ABSTRACT, if different from Report) Unclassified | | |
| 19. SUPPLEMENTARY NOTES | | |
| 20. KEY WORDS (Continue on reverse side if necessary and identify by block number) Clays Soft soils Embankments Soil deformation Pore pressure | | |
| 21. ABSTRACT (Continue on reverse side if necessary and identify by block number) Most soft clays in their natural state exhibit a small degree of overconsolidation resulting from changes in ground water level, delayed consolidation, or other causes. The overconsolidation ratio is commonly in the range of 1.0 to 2.5. Under surface loading, pore pressures in such a deposit will develop as for an elastic material until the effective stresses reach a yield condition or failure condition. In the latter case the soil can (Continued on p 1473 B) | | |

DD FORM 1 JAN 73 1473 EDITION OF 1 NOV 65 IS OBSOLETE

Unclassified

SECURITY CLASSIFICATION OF THIS PAGE (When Data Entered)

038 100

Unclassified

SECURITY CLASSIFICATION OF THIS PAGE(When Data Entered)

20. ABSTRACT (Continued).

continue to carry additional total stresses within confined zones and pore pressures in these zones will continue to increase. In the former case the soil will continue to deform plastically until it reaches failure, showing, in general, different pore pressure responses in these two phases. Thus pore pressure response at any point in a soft clay deposit under increasing surface loading may show two or three distinct phases, although in some cases the plastic and failure responses may be almost indistinguishable. In this report, three published field records ~~are examined~~. One of these, a circular embankment loading on sensitive clay, is studied in some detail and it is found that at the end of the initial elastic phase, contained failure occurs with a distinct change in pore pressure response with further loading. The plastic phase is absent. In the second case, again a circular embankment but on soft clay of comparatively low sensitivity, the pore pressure response under loading is distinctly three-phased. In the final case record studied, a road embankment loading on Boston blue clay, a distinct change in pore pressure response occurs at the end of the elastic phase, followed by a phase in which plastic yielding if it occurs is not clearly distinguishable from the contained failure response.

1473B

Unclassified

SECURITY CLASSIFICATION OF THIS PAGE(When Data Entered)

FOREWORD

The investigation described herein was one phase of a project, "Instrumentation of Embankments and Foundations," sponsored by the Office, Chief of Engineers (OCE), under CWIS 31129. The investigation was conducted during the period January 1975 through July 1976.

The general objective of this study was to present the interpretation of field records for the yield conditions associated with pore pressure responses in soft soils under surface loading. Work on this project was conducted and the report was prepared by Professors R. H. G. P.rry, Lecturer, University of Cambridge, England, and C. P. Wroth, Reader in Soil Mechanics, University of Cambridge, England.

The contract was monitored by Mr. C. L. McAnear, Chief, Soil Mechanics Division, under the general supervision of Mr. J. P. Sale, Chief, Soils and Pavements Laboratory. Contracting Officer was COL G. H. Hilt, Director of the Waterways Experiment Station.

| | |
|---------------------------------|---|
| ACCESSION FOR | |
| DTIC | Write Section <input checked="" type="checkbox"/> |
| DOC | Diff Section <input type="checkbox"/> |
| UNANNOUNCED | <input type="checkbox"/> |
| JUSTIFICATION | |
| BY | |
| DISTRIBUTION/AVAILABILITY CODES | |
| Dist. | AVAIL. AND SPECIAL |
| A | |

DDC
RECEIVED
OCT 19 1976
D

CONTENTS

| | | Page |
|-----|--|------|
| 1 | Introduction | 1 |
| 2 | Application to field case of axisymmetric loading at Åsrum | 2 |
| 2.1 | General description | 2 |
| 2.2 | Åsrum 1. Piezometer A at 3 m depth on the centre line | 3 |
| 2.3 | Åsrum 1. Piezometer E at 5 m depth on the centre line | 6 |
| 2.4 | Åsrum 1. Piezometers not on the centre line | 7 |
| 3 | Application to field case of axisymmetric loading at Canvey Island | 8 |
| 4 | Application to field case of plane strain loading near Boston, Mass. | 9 |
| 5 | Conclusions | 11 |
| | References | 12 |

Figs. 1-12

Appendix: A

"Field loading test at Canvey Island" by George P.J. and Parry R.H.G.

"The response of a soft clay layer to embankment loading" by Pender M.J., Parry R.H.G. and George P.J.

PORE PRESSURES IN SOFT GROUND UNDER SURFACE LOADING

1. Introduction

In the first of this pair of reports, theories were developed for the excess pore pressures that would be developed in soft clay as a result of surface loading. It was shown that most deposits of soft clay will be in a lightly overconsolidated state (as a result of desiccation, lowering and raising of the water table or delayed consolidation). For a typical element, P in Fig.1(a) at depth z in a deposit of soft clay, the existing effective stresses acting on the element are σ'_v , $\sigma'_h = K_0 \sigma'_v$. The total and effective stress states of the element are shown as points P and P' in Fig.1(b) in terms of the parameters:-

the mean total principal stress $p = \frac{1}{3}(\sigma_1 + \sigma_2 + \sigma_3) = \frac{1}{3}(\sigma_v + 2\sigma_h)$

the mean effective principal stress $p' = \frac{1}{3}(\sigma'_1 + \sigma'_2 + \sigma'_3) = \frac{1}{3}(\sigma'_v + 2\sigma'_h)$

the deviator stress $q = (\sigma'_1 - \sigma'_3) = (\sigma'_v - \sigma'_h)$

It was shown that the typical total and effective stress paths for the element caused by some surface loading would be PQRS and P'Q'R'S' with the response of the element displaying three distinct phases. These phases would be:-

- (i) an 'elastic' response P'Q'
- (ii) a plastic phase Q'R' and
- (iii) contained failure R'S'.

The excess pore pressures which would be generated in the element, are shown qualitatively in Fig.1(c) in which Δu has been plotted against the increment of total vertical stress $\Delta \sigma_v$ (local) experienced by the element as a consequence of the surface loading. Expressions for the gradients of the three linear portions of the plot of Fig.1(c) are given in the first report.

In this second report, these theoretical ideas of pore pressure development are applied to well documented field cases.

The first case is that of axisymmetric loading of two circular fills at Åsrum, in Norway, reported by Høeg, Andersland and Rolfsen (1969). The other case are of an axisymmetric loading at Canvey Island, England reported by Pender, Parry and George (1975) and of a plane strain case of a long road embankment at Boston reported by D'Appolonia, Lambe andoulos (1971).

2. Application to Field Case of Axisymmetric Loading at Åsrum

2.1 General Description

In order to study the problems of likely settlement of buildings on the quickclays in the area around Oslo, the Norwegian Geotechnical Institute carried out two field tests on a site at Åsrum. Each test consisted of a circular fill placed on the existing ground surface, with careful measurements being made of excess pore pressures generated in the underlying clay, and of settlements of the fill. Full details are given by Høeg, Andersland and Rolfsen (1969).

Profiles of the soil at the two neighbouring sites, are given in Fig.2a, and the in situ vertical stresses in Fig.2b (both diagrams being reproduced from the paper by Høeg et al.). The upper 1 to 2 m consists of a fairly stiff fissured crust, below which the very quick and soft clay extends to bedrock. The natural water content of the clay ranges from about 55% to 70% compared to a range of liquid limits of about 35% to 50%. The undrained shear strength was measured by in situ vane tests and unconfined compression tests on undisturbed samples. Beneath the surface crust the strength is as low as 0.5 tonne/m² (50 kN/m²) and it increases with depth.

The observed values of the excess pore pressures recorded by the piezometers at depths of 3 m and 5 m beneath the two fills are shown in Figs.3a to 3d. It is at once apparent that the responses of the piezometers near the centreline show two well defined phases, with a sharp break between the two phases. These responses will now be interpreted in the light of the theories developed in the first report.

2.2 ^o Asrum I : Piezometer A at 3 m depth on the centre line

The positions of the various piezometers are indicated in Fig.4a. In this section the response of piezometer A at a depth of 3 m on the centre line of the fill is examined in detail.

Since the piezometer is on the centre line, conditions of axial symmetry apply throughout the test. Although the diameter of the fill reduces with height, for the purposes of the calculations the surface loading produced by the fill is assumed to be a uniform circular vertical load of intensity $\Delta\sigma = \gamma h$ and of average radius $a = 6.25$ m as shown in Fig.4b.

For the initial analysis of the behaviour of the soft clay it is assumed that the elastic response is isotropic. From the elastic stress distributions for a uniform flexible circular load of radius a on an elastic half space tabulated by Poulos and Davis (1974) the curves of Fig.5 have been produced. Using these results the relevant values for piezometer A are as follows:-

$$r/a = 0, \quad z/a = 0.48, \quad \Delta\sigma_v/\Delta\sigma = 0.919, \quad \Delta\sigma_h/\Delta\sigma = 0.391 \quad \dots (1)$$

$$\text{Hence the ratio of increments of total stress } \ell_1 = \frac{\Delta\sigma_h}{\Delta\sigma_v} = \frac{0.391}{0.919} = 0.425$$

and the factor $\frac{1}{3}(1 + 2\ell_1) = 0.617$. From eqn.(17) of the first report the perfectly elastic response of piezometer A would be

$$\frac{\Delta u}{\Delta\sigma_v} = \frac{1}{3}(1 + 2\ell_1) = 0.617. \quad (\text{Fig.4c}) \quad \dots (2)$$

In terms of the observed surface load $\Delta\sigma$, (rather than the unknown local increment of total vertical stress $\Delta\sigma_v$) the response is given by $\frac{\Delta u}{\Delta\sigma} = \frac{\Delta u}{\Delta\sigma_v} \cdot \frac{\Delta\sigma_v}{\Delta\sigma} = 0.617 \times 0.919 = 0.567 \quad \dots (3)$
(Fig.4d)

This gradient almost exactly matches that of the first linear portion P'Q' of the relevant plot in Fig.3*. The point Q corresponds to the change in behaviour from an elastic response

* It should be noted that the scales in Figs.3a to 3d for Δu and $\Delta\sigma$ are unfortunately not the same.

to either a plastic response or contained failure. This occurs at an increment of surface load of $\Delta\sigma = 2.84 \text{ tonne/m}^2$ (285 kN/m^2) for which the excess pore pressure generated at piezometer A based on an elastic response would be from eqn.(3)
 $\Delta u = 0.567 \Delta\sigma = 1.61 \text{ t/m}^2$. This corresponds closely to the value observed for point Q in Fig.3.

If the clay behaves perfectly elastically in the first phase then the excess pore pressure is given directly by the increment of mean total principal stress Δp as shown below:

$$\Delta p = \frac{1}{3}(\Delta\sigma_v + 2\Delta\sigma_h)$$

$$\Delta p' = \frac{1}{3}[(\Delta\sigma_v - \Delta u) + 2(\Delta\sigma_h - \Delta u)]$$

$$\therefore \Delta p - \Delta p' = \Delta u$$

In an isotropic elastic soil under undrained conditions (i.e. no volume change) $\Delta p' = 0$ and the stress path on a q - p' plot is a vertical straight line (see p 10 first report).

Thus, if $\Delta p' = 0$

$$\Delta u = \Delta p$$

Hence the result of eqn.(3) could be obtained directly from the appropriate curve for $\Delta p/\Delta\sigma$ in Fig.5, without the need to calculate the stress increments $\Delta\sigma_v$ and $\Delta\sigma_h$. But evaluation of the latter has two advantages:- (i) it allows estimates to be made of the total and effective stress paths and hence a fuller understanding of the behaviour of the clay, and (ii) it allows an anisotropic elastic response of the clay to be used, if necessary, i.e. the use of the expressions given in eqn.(17) and table 1 of the first report.

At the stage represented by Q' the clay locally around piezometer A yields. At yield, then, $\Delta\sigma = 2.84 \text{ t/m}^2$. From elastic theory $\Delta\sigma_v = 2.61$, $\Delta\sigma_h = 1.11$, $\Delta p' \equiv 0$

$$\Delta q = 1.50, \Delta p = 1.61 \text{ (all units : t/m}^2\text{)}$$

.. (4)

The total and effective stress paths for the stages PQ and P'Q' can now be plotted if the initial in situ stress states are known. Unfortunately the problem of the in situ lateral stress is a difficult one, and the best that can be done is to estimate this from all the limited information available.

From the results of the consolidation tests and the profile of stresses in Fig.2b, for the depth $z = 3$ m, $\sigma'_{v0} = 1$ t/m², $u_0 = 4.5$ t/m² and the overconsolidation ratio is 3. Making use of eqn.(6) in the first report for estimating the value of K_0 for lightly overconsolidated soils

$$K_0 = OCR K_{n.c.} - \frac{v'}{1-v'} (OCR-1) \quad \dots (5)$$

and taking $K_{n.c.} = 0.65$ and $v' = 0.28$ (for a soil with plasticity index of 16%), then

$$K_0 = 3 \times 0.65 - \frac{0.28 \times 2}{0.72} = 1.26$$

Adopting this estimate for K_0 gives $\sigma'_{ho} = 1.26$ $\sigma'_{v0} = 1.00$ t/m², $q_0 = -0.26$ t/m², $p'_0 = 1.17$ t/m² and $p_0 = 5.67$ t/m². The total and effective stress paths $P_A Q_A R_A$ and $P'_A Q'_A$ for an element of soil at point A based on these estimated in situ stresses are plotted in Fig.6. From the position of the point Q'_A , and from the in situ vane shear strengths (plotted in Fig.2a) of about 0.8 t/m² corresponding to $q_f = 1.6$ t/m², it is concluded that the clay has probably reached failure at point Q'_A . This will mean that for the soil at this depth of 3 m there will be no second phase of plastic yielding (i.e. R' in Fig.1c coincides with Q') and that the behaviour goes directly from elastic to contained failure.

If this suggestion is correct then the second linear phase of pore-pressure response in Fig.3a should have a gradient $\Delta u / \Delta \sigma = \Delta \sigma_v / \Delta \sigma$ assuming that no post-peak softening occurs (see section 9.3 of the first report). Once the clay has yielded or failed the assumption of an elastic stress distribution throughout the elastic half-space is no longer valid. But most of the soil, some distance from the region of contained failure, is still behaving elastically; inside the failing region the total stress distribution must alter to some degree to accommodate the plastic strains of the soil. There is limited evidence to show that the increments of total vertical stress $\Delta \sigma_v$ remain as

though they were given by elastic theory and the increments of total horizontal stress $\Delta\sigma_h$ are larger than the corresponding elastic values. If it is assumed for the sake of argument that the elastic stress distribution for $\Delta\sigma_v$ is valid then for the phase R'S', the expected response is $\frac{\Delta u}{\Delta\sigma} = \frac{\Delta\sigma_v}{\Delta\sigma} = 0.919$.

The observed value is 1.03, so that the above assumptions are in reasonable agreement with the field data, and certainly do not conflict with them. It seems likely, in fact, that some post-peak softening occurred.

2.3 Assum I : Piezometer E at 5 m depth on the centre line

Adopting the same assumptions for piezometer E as for piezometer A the relevant values are as follows:-

$$r/a = 0, \quad z/a = 0.8, \quad \Delta\sigma_v/\Delta\sigma = 0.756, \quad \Delta\sigma_h/\Delta\sigma = 0.184 \quad \dots (6)$$

$$\text{Therefore} \quad \lambda_1 = \frac{0.184}{0.756} = 0.243$$

$$\frac{\Delta u}{\Delta\sigma_v} = \frac{1}{3}(1 + 2\lambda_1) = 0.496 \quad \dots (7)$$

$$\text{and} \quad \frac{\Delta u}{\Delta\sigma} = 0.496 \times 0.756 = 0.375$$

This gradient should be compared to that of 0.45 for the observed data of Fig.3b.

At yield $\Delta\sigma = 3.1 \text{ t/m}^2$ and from elastic theory

$$\left. \begin{aligned} \Delta\sigma_v &= 2.34 & \Delta\sigma_h &= 0.57 & \Delta p' &= 0 \\ \Delta q &= 1.77 & \Delta p &= 1.16 & (\text{all units : t/m}^2) \end{aligned} \right\} (8)$$

An estimate is now made of the initial in situ stress state at E, on the same basis as for A in the last section. From Fig.3, for $z = 5 \text{ m}$, $\sigma'_{v0} = 1 \text{ t/m}^2$, $u_0 = 7.7 \text{ t/m}^2$ and OCR = 3. As before K_0 is taken as 1.26 so that $\sigma'_{h0} = 1.26 \text{ t/m}^2$, $q_0 = -0.26 \text{ t/m}^2$, $p'_0 = 1.17 \text{ t/m}^2$ and $p_0 = 8.87 \text{ t/m}^2$. The total and effective stress paths $P_E Q_E R_E$ and $P'_E Q'_E R'_E$ for an element of soil at E are plotted in Fig.6; the effective stress path starts from the same point as for element A (by chance) and only differs

from it by virtue of a slightly larger value of Δq to cause yield.

The same argument as for element A is invoked to suggest that element E has reached failure at Q_E^* , and that the behaviour of the soil changes directly from elastic to contained failure without an intermediate stage of plastic yielding.

On this basis the gradient of the second stage would be expected to be $\frac{\Delta u}{\Delta \sigma} = \frac{\Delta \sigma_v}{\Delta \sigma} = 0.756$; this compares with a measured value of 0.687 from Fig.3h.

2.4 Figure 1 : Piezometers not on the centre line

For the piezometers B,C,D at 3 m depth and F,G,H at 5 m depth not on the centre line of the fill conditions of axial symmetry no longer apply. The simple expressions derived in the first report are not valid, and the situation is much more complicated because of the rotation of the principal axes of stress and stress increment.

However if the soil behaves in an isotropic elastic manner while undergoing no volume change, then $\Delta p' \equiv 0$ and the excess pore pressure is given (as before) by the increment of mean total principal stress Δp . From the charts and functions given by Poulos and Davis (1974) the ratios $\Delta p/\Delta \sigma$ have been calculated for the six piezometers, and are compared in table 1 with the observed gradients of $\Delta u/\Delta \sigma$ taken directly from the first phases of the responses plotted in Figs.3a and 3b. There is reasonably good agreement between the two sets of values, which supports the interpretation of the results in terms of isotropic elasticity.

| Piezometer | z/a | r/a | Computed $\Delta p/\Delta \sigma$ | Observed $\Delta u/\Delta \sigma$ |
|------------|------|-----|--------------------------------------|--------------------------------------|
| A | 0.48 | 0 | 0.567 | 0.600 |
| B | 0.48 | 0.4 | 0.532 | 0.546 |
| C | 0.48 | 0.8 | 0.396 | 0.343 |
| D | 0.48 | 1.2 | 0.186 | 0.105 |
| E | 0.8 | 0 | 0.375 | 0.45 |
| F | 0.8 | 0.4 | 0.347 | 0.315 |
| G | 0.8 | 0.8 | 0.266 | 0.276 |
| H | 0.8 | 1.2 | 0.162 | 0.150 |

Table 1 Comparison between first phase of the observed excess pore pressures and those computed from elastic theory.

The consequences of the departure from the simple case of axial symmetry is illustrated for the case of piezometer G in Fig.7. From Poulos and Davis (1974) it is possible to calculate the increments of stress shown in perspective in Fig.7a and in elevation in Fig.7b from elastic theory in terms of the applied (circular) surface load $\Delta\sigma$. They are $\Delta\sigma_z/\Delta\sigma = 0.504$, $\Delta\sigma_r/\Delta\sigma = 0.185$, $\Delta\sigma_\theta/\Delta\sigma = 0.109$, $\Delta\tau_{rz}/\Delta\sigma = 0.204$. The Mohr's circle of stress for the (r,z) plane is shown in Fig.7c, and the principal increments of stress can readily be calculated to be

$$\Delta\sigma_1/\Delta\sigma = 0.603, \quad \Delta\sigma_2/\Delta\sigma = \Delta\sigma_3/\Delta\sigma = 0.109, \quad \Delta\sigma_3/\Delta\sigma = 0.086$$

The principal axes of the stress increments are as shown in Fig.7d and do not coincide with those of stress (the principal directions of which depend on the ratio of $\Delta\sigma$ to the initial in situ stresses at point G).

After yield has occurred, which is assumed to coincide with the onset of contained failure, the local distribution of stresses in the vicinity of G can no longer be elastic. It is suggested for want of any experimental evidence that the distribution of the major principal stress increment $\Delta\sigma_1$ remains largely unaffected and that $\Delta u = \Delta\sigma_1$. If this hypothesis is valid then the expected gradient in Fig.3a for the second phase for piezometer G would be $\frac{\Delta u}{\Delta\sigma} = \frac{\Delta u}{\Delta\sigma_1} \cdot \frac{\Delta\sigma_1}{\Delta\sigma} = 0.603$. This should be compared with an observed value of about 0.5.

3. Application to Field Case of Axisymmetric Loading at Canvey Island

As part of a detailed site investigation for a major oil refinery on a deposit of soft clay at Canvey Island in England, two small circular trial embankments were constructed to simulate the behaviour of the oil tanks. The performance of the embankment was monitored by observations of the settlement of the embankment, and of excess pore pressures recorded by piezometers placed in the ground beneath.

A detailed description of the site and instrumentation is given by George and Parry (1973). The pore pressure responses have been interpreted by Pender, Parry and George (1975) in the light of the theories advanced in the first report. These papers are appended to this report, and their main findings only will be presented briefly here.

Undisturbed samples of the soft clay were subjected to stress controlled drained triaxial tests with a variety of stress paths in order to establish the yield locus. The results are shown in Figs.13 and 14 of the first of this pair of reports.

The locations of four piezometers, P1, P5, P7 and P10 are given in Fig.8. Observed pore pressure changes are plotted in Fig.9 against changes in vertical total stress $\Delta\sigma_v$ at tip level calculated by finite element analysis using a bilinear model. The response of each piezometer shows the expected pattern of three linear phases, with well defined points of change between the phases. For the first phase of the pore-pressure response the resulting value of the ratio $\Delta u/\Delta p$ was 0.5 to 0.6 whereas that predicted from isotropic elasticity would be 1. However this discrepancy may be due to any or all of the following reasons:-

- (i) the soil may contain gas in the pore water due to the organic matter present in a recent alluvial deposit,
- (ii) the soil may behave anisotropically,
- (iii) the excess pore pressures will be dissipating during the period of the construction of the embankment,
- (iv) the finite element computations are only approximate and are affected by the choice of boundary conditions and distribution of soil parameters within the mesh of elements.

4. Application to Field Case of Plane Strain Loading near Boston, Mass.

A well documented case history for the plane strain situation is reported by D'Appolonia, Lambe and Poulos (1971). The paper reports the evaluation of excess pore pressures measured

under a long road embankment constructed near Boston as part of the Interstate Highway system.

A cross section of the embankment is shown in Fig.10a and piezometer locations in Fig.10b. Full details of the properties of the ground are given in the paper by D'Appolonia et al. A selection of the observed values of excess pore pressure is shown in Fig.11 where the results are plotted against the elevation of the embankment.

All the piezometer readings show two distinct responses. The end of the elastic phase is clearly defined in each case, as the local element of soil (around the piezometer) yields plastically or fails after behaving elastically. It was pointed out in Section 9.3 of the first report that in some cases the pore pressure responses in phases 2 and 3 (i.e. plastic yielding and failure) would be difficult to distinguish. It can be seen that some of the responses in Fig.11 could be three phased, although a third phase is not clearly distinguishable. It is possible then that after completion of the elastic phase the soil did progress through a plastic phase to contained failure without any distinct change in pore pressure response.

D'Appolonia et al have made great efforts to interpret these results and they have considered four different distributions of increment of total stresses. They have also considered various relationships between changes of total stress and of pore pressures. They conclude that for the pre-yield elastic phase the best prediction of pore pressure is given by three-dimensional elastic theory (as applied to the plane strain case) with $\Delta u = \Delta p$.

A direct comparison of the ratio of measured to predicted pore pressures (which is directly proportional to the gradients of the first phases shown in Fig.11) is given in Fig.12a for many of the piezometers. Those piezometers near the upper sand layer or near the till showed a substantial degree of dissipation due to drainage and were discounted by D'Appolonia et al.

During contained perfectly plastic failure it has been shown that the change of pore pressure Δu is expected to be

equal to the (local) change of vertical total stress $\Delta\sigma_v$ (local). Values of the ratio $\Delta u/\Delta\sigma_v$ for the same set of piezometers were calculated by D'Appolonia et al, and are reproduced in Fig.12b. The values are all greater than unity, but generally close to it. The underpredictions indicate either that, as suggested above, the soil after local yield progresses through a plastic stage before the onset of local failure (a response of $\Delta u/\Delta\sigma_v > 1$ is possible in the plastic phase) or that a small degree of post peak softening occurring in the soil as discussed in Section 9.4 of the first report.

6. Conclusions

The theoretical considerations of pore pressures generated in soft ground by surface loading have been compared with three well documented case histories.

In all three cases - two axially symmetric, one plane strain - the pore pressure responses recorded by piezometers were linearly related to the applied surface loading. As expected the response had two or three stages: an initial elastic phase followed by plastic yielding and/or contained failure.

For the first case of the circular fill at Åsrum, which was studied in detail, the total and effective stress paths were estimated for the locations of two of the piezometers. These paths confirmed that the clay was sufficiently overconsolidated (albeit to a small degree) that the middle phase of work-hardening plastic behaviour was absent.

The pore pressure responses from the Canvey Island tests showed three distinct phases while the responses from the road embankment test at Boston showed two distinct phases, but it is possible that the second phase combines plastic yielding and contained failure.

In detail, the predictions of pore pressures based on isotropic elastic theory generally appear to overestimate the observed values for the elastic phase by between 20-50%. Part

of this discrepancy can be attributed to anisotropy, to incomplete saturation, or to partial dissipation due to drainage.

The predictions of the pore pressure after yield appear to underestimate the observed values by 10-20% since no allowance has been made for strain softening after failure has occurred. In addition the assumption that the distribution of the total vertical stress is unaffected by inelastic behaviour is questionable, and is based on slender evidence. It is possible that complex finite element computations could resolve this doubt.

The concept of a yield locus for undisturbed samples and its use in the interpretation of pore pressures observed in soft ground under surface loading has been confirmed. For engineering purposes, adequate predictions of pore-pressures may be made by applying the concepts and theories proposed in the first of this pair of reports.

References

- D'Appolonia D.J., Lambe T.W. and Poulos H.G. (1971) 'Evaluation of Pore Pressures Beneath an Embankment' Proc.ASCE Vol.97 SM6 pp 881-897.
- George P.J. and Parry R.H.G. (1973) 'Field Loading Tests at Canvey Island' Proc.Symp. on Field Instrumentation in Geotechnical Engineering pp 152-165, Butterworth, London.
- Høeg K., Andersland O.B. and Rolfsen E.N. (1969) 'Undrained Behaviour of Quick Clay under Load Tests at Åsrum' Geotechnique 19, 101-115.
- Parry R.H.G. and Wroth C.P. (1976) 'Pore Pressures in Soft Ground under Surface Loading: Theoretical Considerations' Report prepared for USAE Waterways Experiment Station.
- Pender M.J., Parry R.H.G. and George P.J. (1975) 'The Response of a Soft Clay Layer to Embankment Loading' Proc 2nd Australia-New Zealand Conference on Geomechanics, pp 169-173, Brisbane.
- Poulos H.G. and Davis E.H. (1974) 'Elastic Solutions for Soil and Rock Mechanics', Wiley.

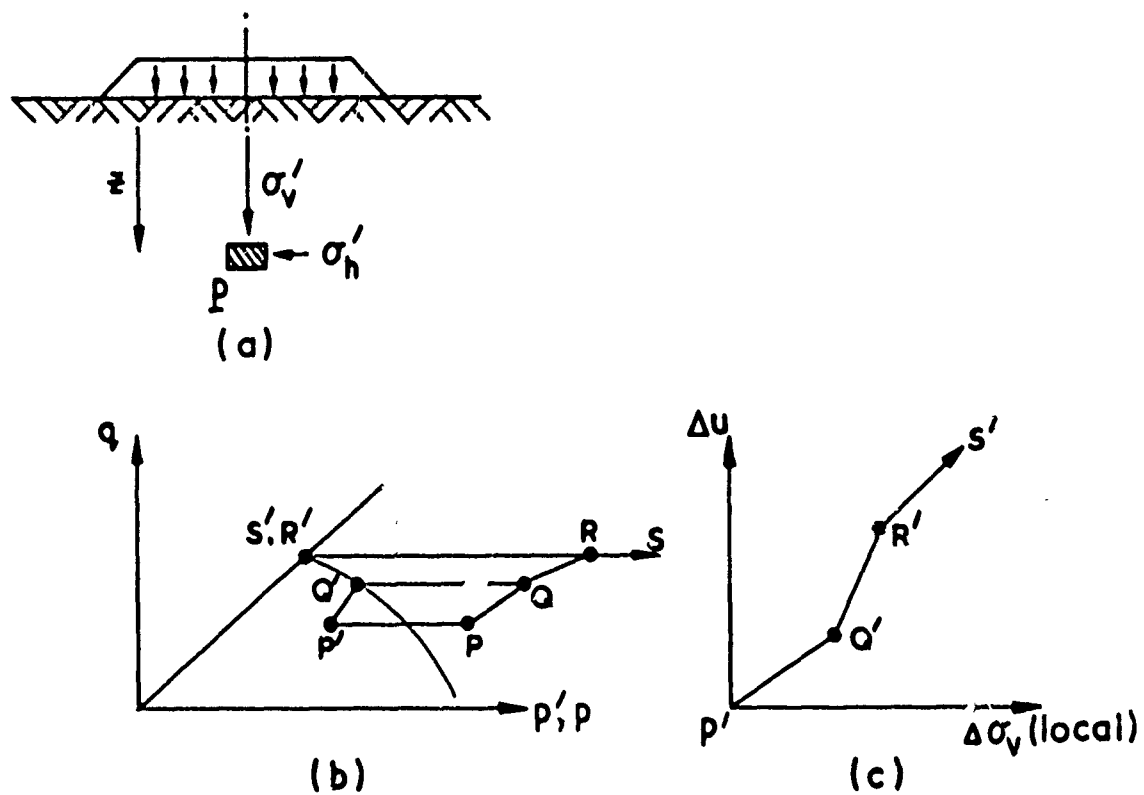
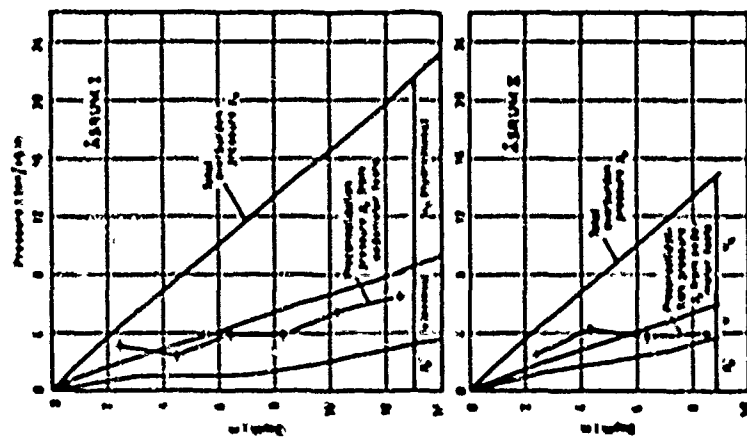
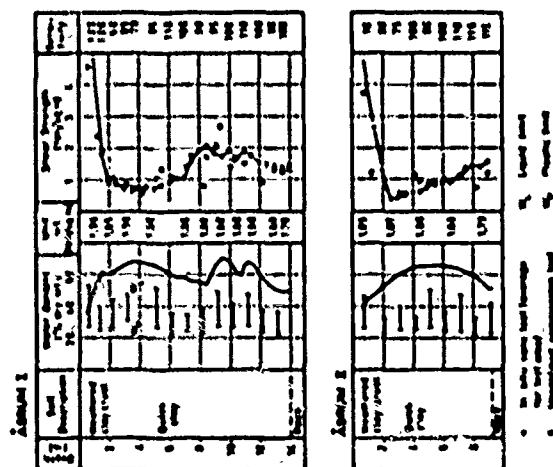


Fig.1 Idealised response of a typical element of soft clay to surface loading (a) location of element (b) effective and total stress paths (c) pore pressure response to change in vertical total stress in element.

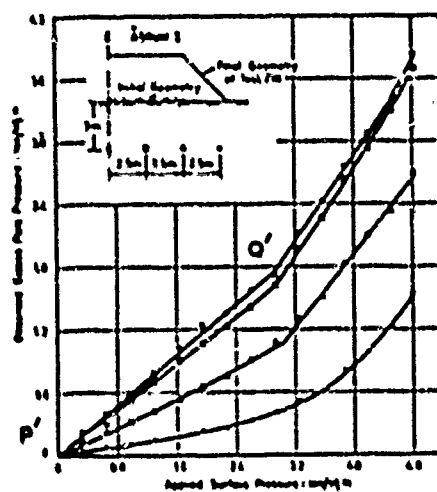


(b)



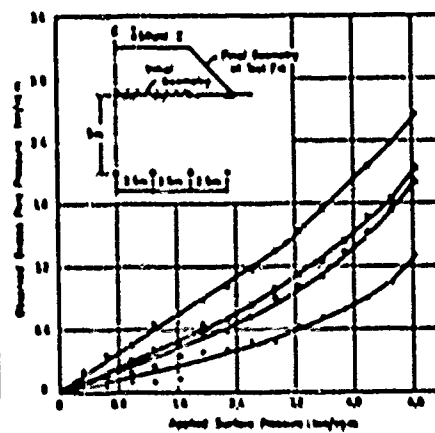
(a)

Fig. 2 Ground conditions at Åsrum site (a) soil profiles (b) in situ stress conditions. (after Høeg, Andersland and Rolfsen, 1969).



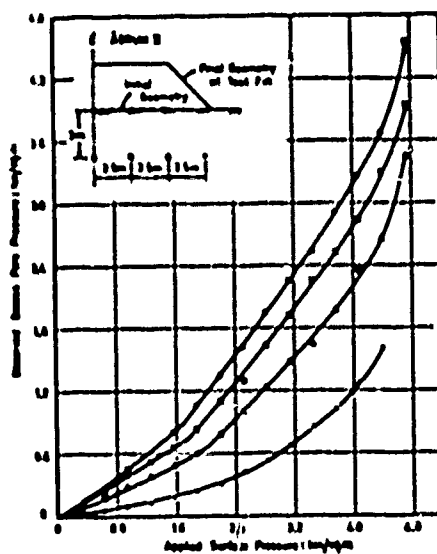
Observed excess pore pressure—
depth 3 m: Åsrum I

(a)



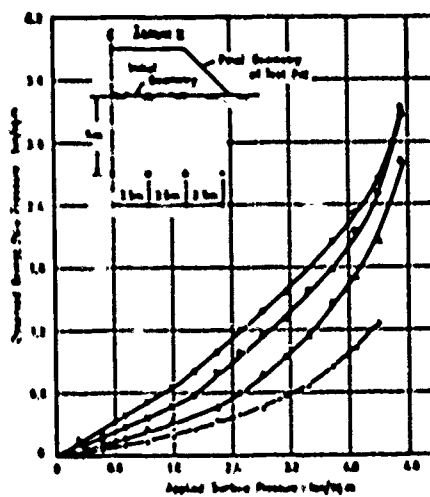
Observed excess pore pressure—
depth 5 m: Åsrum I

(b)



Observed excess pore pressure—
depth 3 m: Åsrum II

(c)



Observed excess pore pressure—
depth 5 m: Åsrum II

(d)

Fig.3

Pore pressure responses at Åsrum 1 and Åsrum 2 sites. (after Høeg, Andersland and Rolfsen).

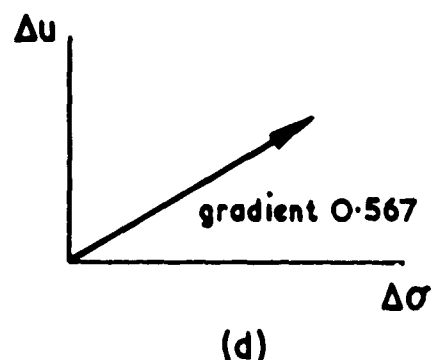
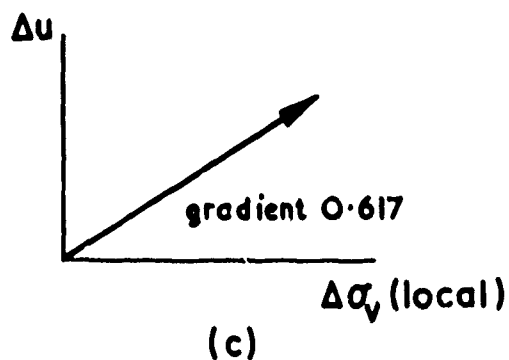
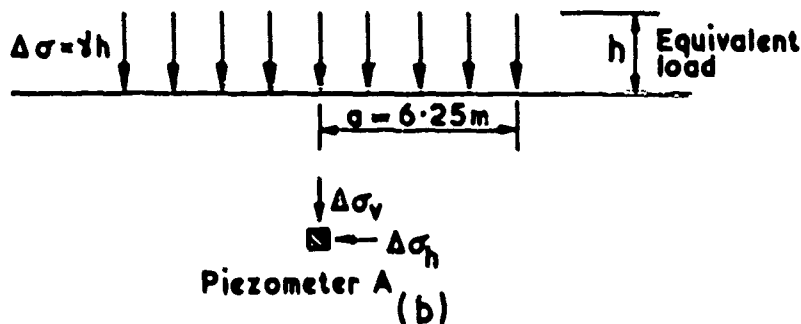
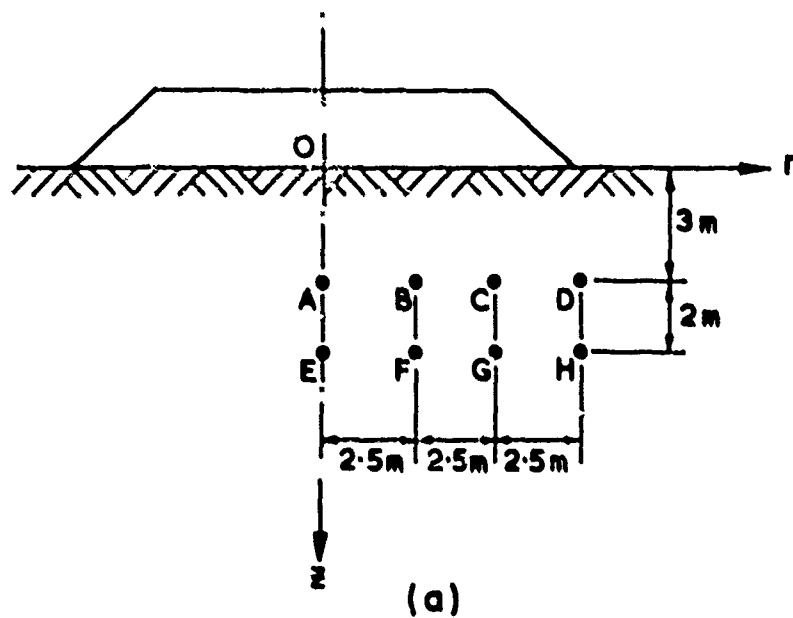


Fig.4 Predicted pore pressure response at Åsrum 1 site
 (a) locations of piezometers (b) idealised equivalent loading (c) elastic pore pressure response for piezometer A related to change in total vertical stress at piezometer tip (d) elastic pore pressure response for piezometer A related to surface loading

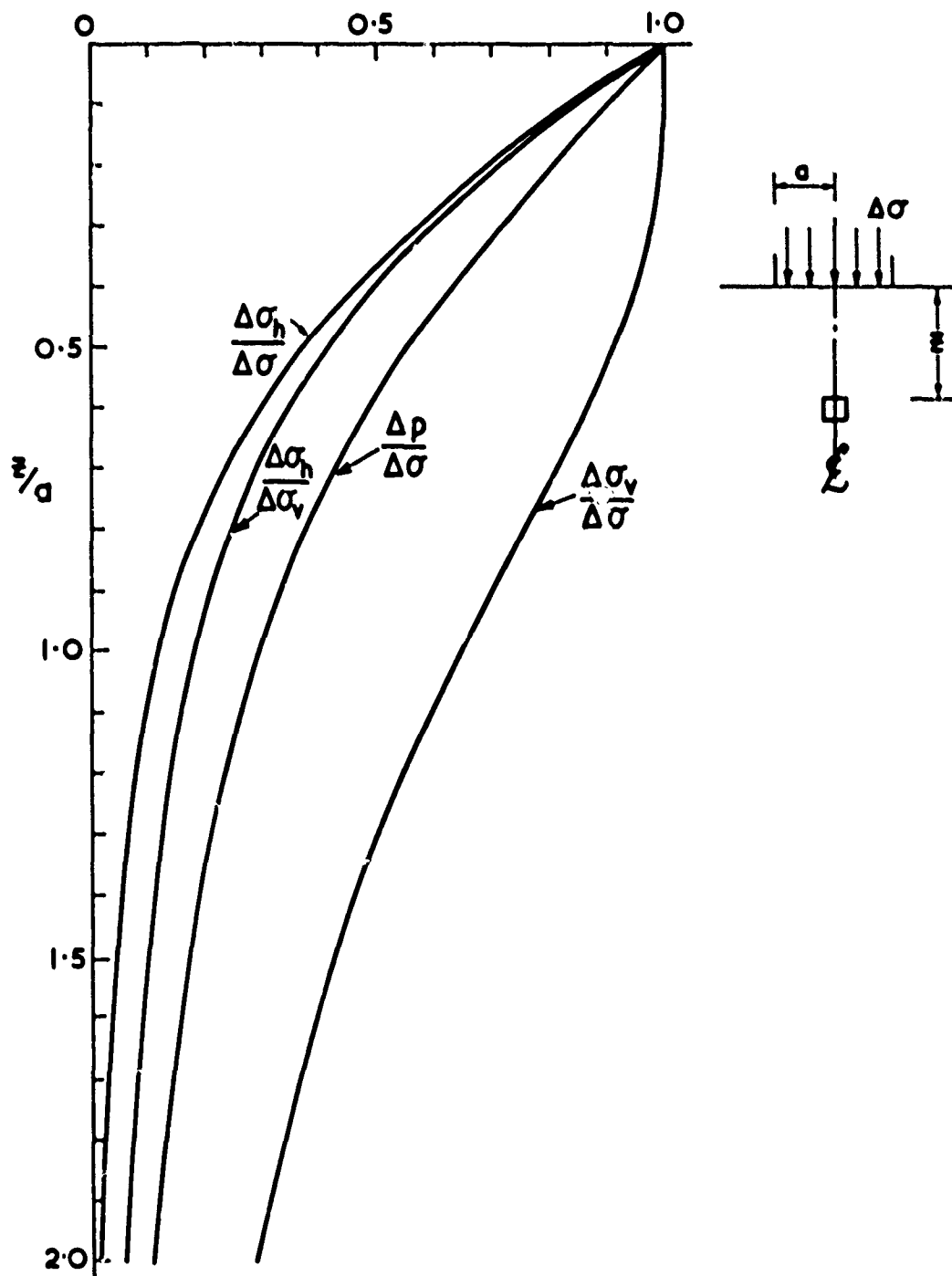


Fig.5 Elastic stress increments on centre line below a uniform circular load.

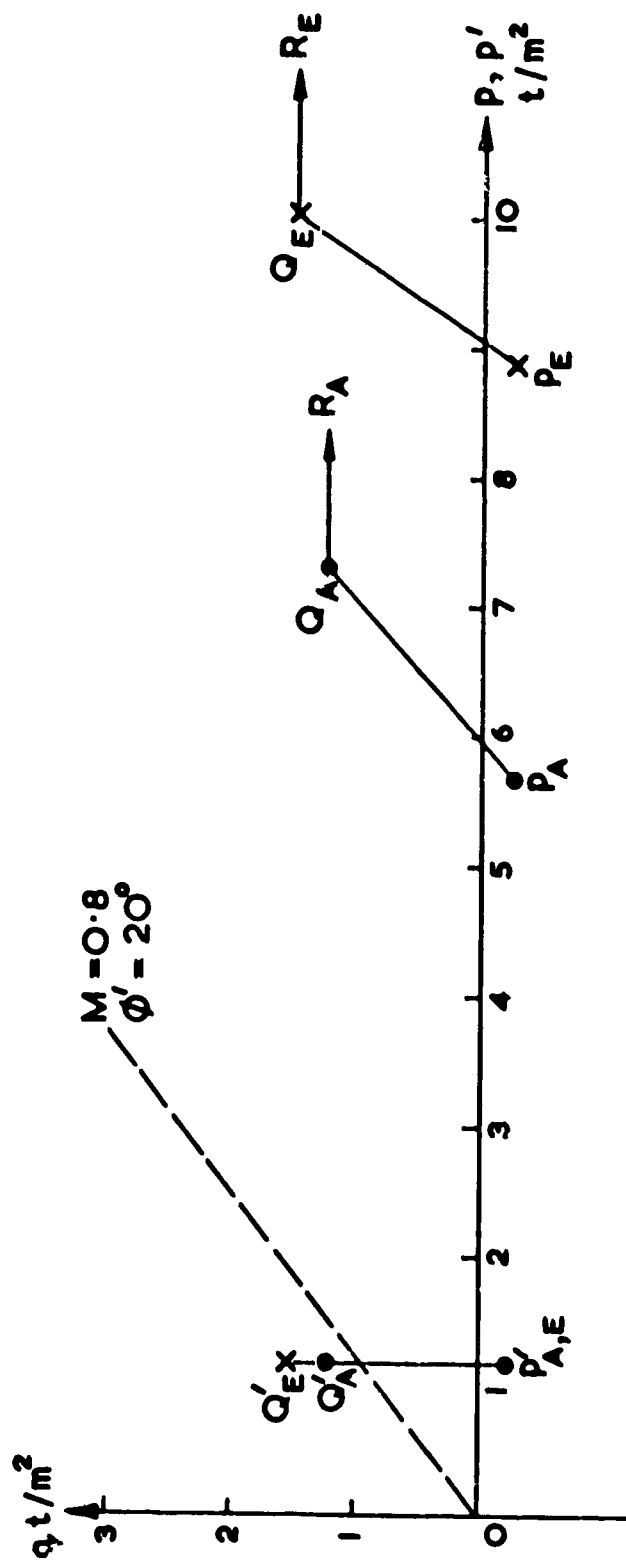


Fig.6 Predicted total stress and effective stress paths for piezometers A and E at Asrum 1 site.

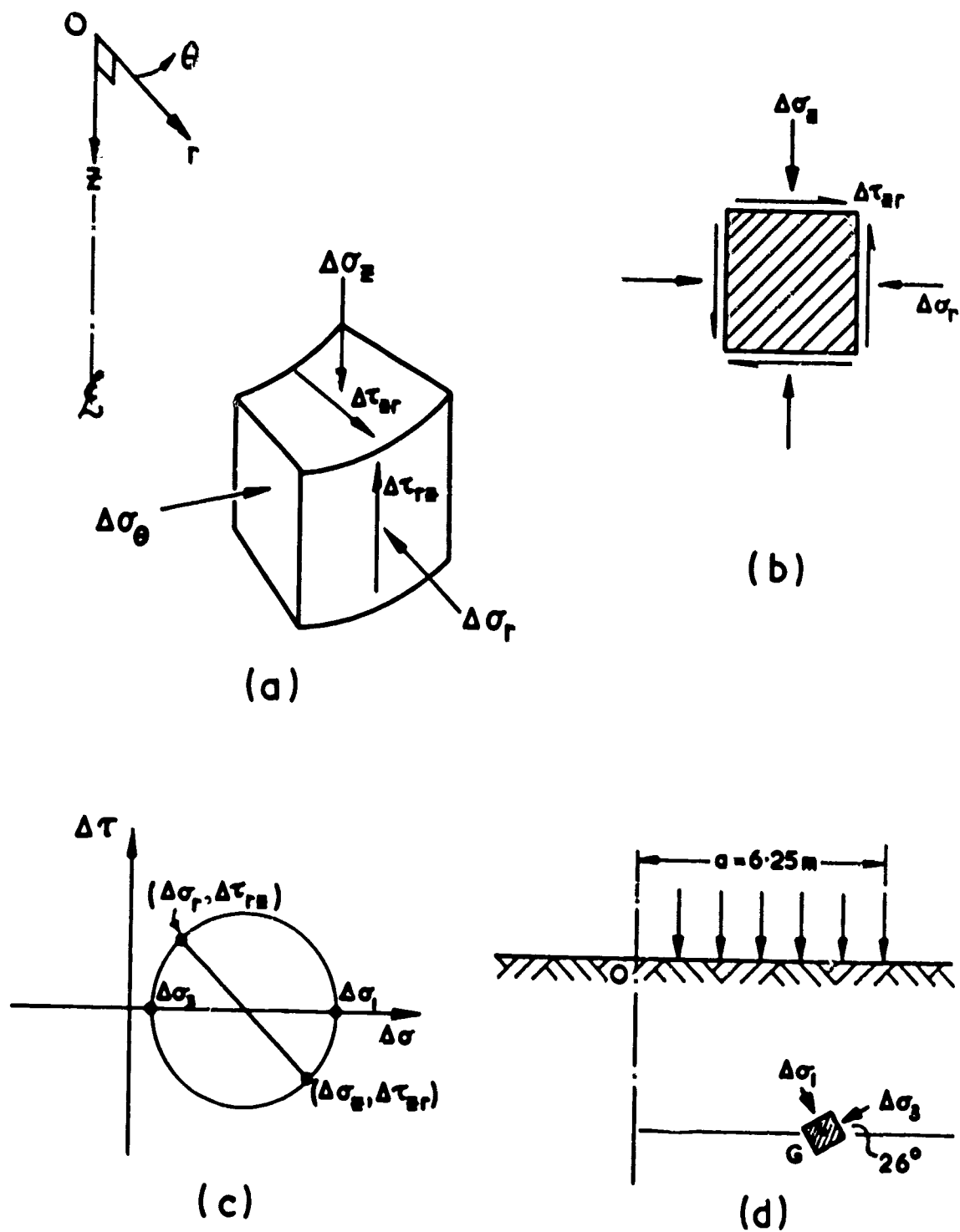


Fig.7

Applied stresses at piezometer G at Åsrum 1 site
 (a) a perspective view and (b) an elevation showing
 total stress increments (c) Mohr circle of total
 stress increments (d) directions of principal total
 stress increments from elastic theory.

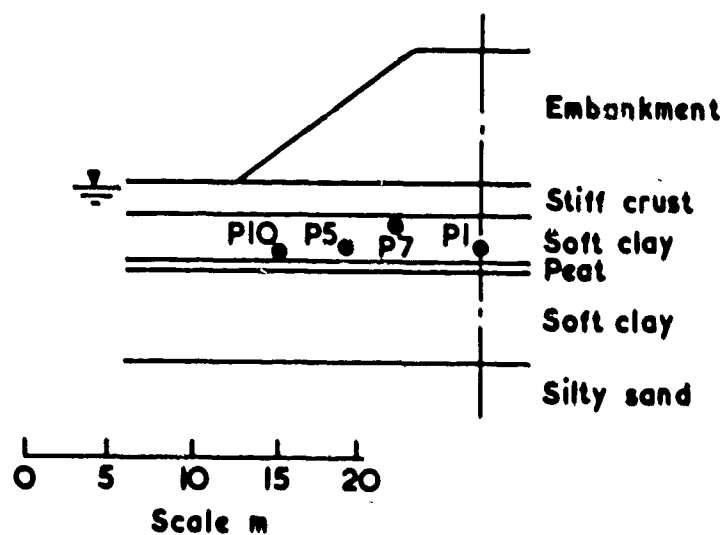


Fig.8 Soil profile and piezometer locations for Canvey Island loading test (after George and Parry 1973).

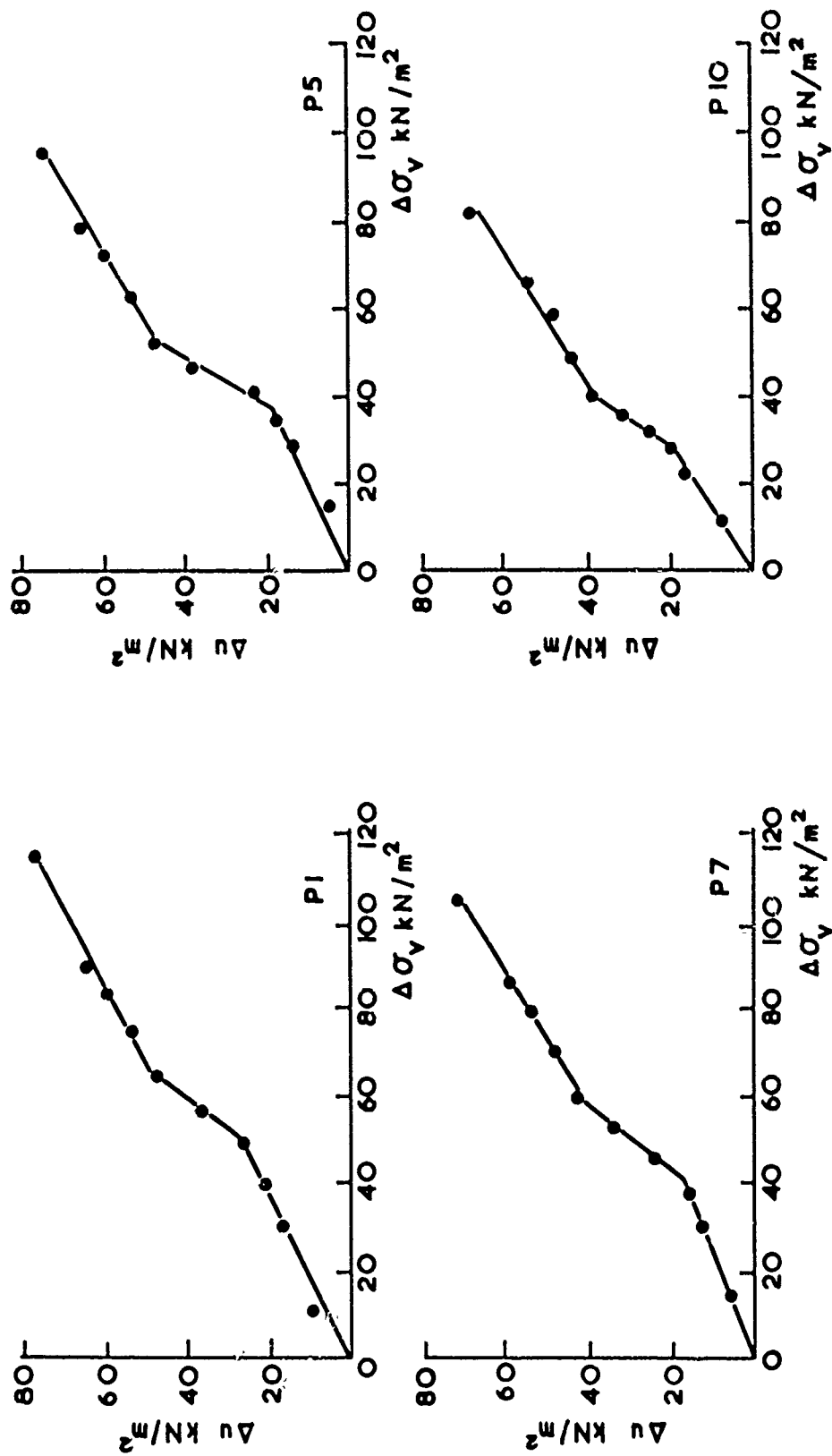
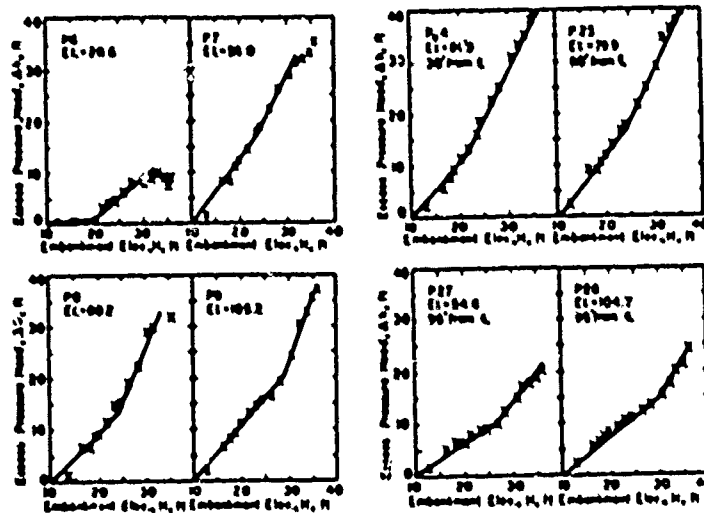


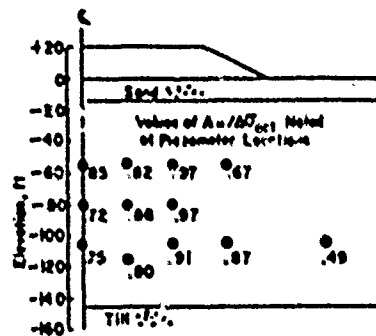
Fig.9 Pore pressure responses for Canvey Island piezometers P1, P5, P7, P10 plotted against calculated value of total vertical stress (after Pender, Parry and George 1975).



EXCESS HEAD AS FUNCTION
OF EMBANKMENT ELEVATION FOR
PIEZOMETERS UNDER CENTER LINE

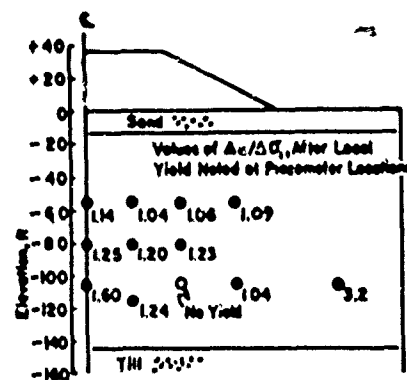
EXCESS HEAD AS FUNCTION
OF EMBANKMENT ELEVATION FOR
PIEZOMETERS OFF CENTER LINE

Fig.11 Piezometer responses under Boston test embankment as a function of embankment elevation (after D'Appolonia, Lanbe and Poulos 1971).



RATIO OF MEASURED PORE PRESSURE TO PORE PRESSURE CALCULATED BEFORE LOCAL YIELD USING THREE-DIMENSIONAL ELASTIC THEORY

(a)



RATIO OF MEASURED PORE PRESSURE TO CALCULATED PORE PRESSURE AFTER LOCAL YIELD

(b)

Fig.12 Pore pressure changes under Boston test embankment (a) before local yield presented as a ratio of measured to calculated values (b) after local yield presented as a ratio of measured values to values calculated by D'Appolonia, Lambe and Poulos.

Appendix: A

"Field loading test at Canvey Island" by
George P.J. and Parry R.H.G.

"The response of a soft clay layer to embankment
loading" by Pender M.J., Parry R.H.G. and George P.J.

FIELD LOADING TESTS AT CAVEY ISLAND

P. J. George

R. M. G. Parry

Dames & Moore

Cambridge University

SYNOPSIS

Field loading tests are being carried out at Cavery Island to provide information for the design of oil storage tanks. The site consists of about 8 m of soft clay overlying dense sand. Two circular embankments were constructed of 30 m diameter and with a planned height of 8.6 m. Sandvicks were placed under one tank only, to determine their value in accelerating pore pressure dissipation. Instrumentation in the soft clay underlying the embankments includes three separate methods of measuring settlements (the results of which are compared) together with inclinometer tubes and piezometer points.

The writers' experience regarding contract problems, usefulness of instrumentation and an evaluation of cost and benefit are also recorded.

INTRODUCTION

It is proposed to construct the Thames Oil Refinery on an undeveloped soft soil site, adjacent to the river Thames at Cavery Island, Essex. The refinery will have a total storage capacity of 1,255,000 m³ for crude oil and petroleum product (120,000 barrels per day).

If local practice were to be followed, high expenditure would be incurred in piling to support the tanks. However, it should be possible to construct limited height ground supported tanks, providing reasonably long water pre-loading programmes are scheduled. Economic and production considerations put a limitation on the maximum period of pre-loading, and thus emphasised the need for confident foundation recommendations, if such a scheme is to be adopted.

A preliminary site investigation had shown that the upper 7

to 15 m of soil were soft, highly compressible and slow draining, but uniform in thickness and characteristics.

To study the feasibility of the scheme, a comprehensive site investigation was put in hand, which included the construction of two comparative embankment load tests.

This paper describes the application of field instrumentation to these trial fills to establish basic design criteria, and to design a full scale tank monitoring scheme. Commercially manufactured instrumentation systems were used throughout.

The embankments were constructed to study the effect of vertical drains as a method of ground treatment. Embankment No. 1 was constructed to a maximum height of 7.3 m without ground treatment. Embankment No. 2 was taken to 8.6 m when a slip occurred. The ground under this embankment was treated with 8.0 m long, 60 mm diameter sandvicks (Castidar and Gupta 1967) installed at 1.5 m and 2.0 m spacing.

The embankments were constructed as circular frustra having base diameters of 30 m, and were separated by 10 m. Circular loading was adopted to simplify analysis (axisymmetric conditions) and simulate tank foundations. In addition a considerable saving in fill material was achieved over equivalent width loads adopting square or rectangular constructions.

If ground treatment were to be recommended as a result of the trials the possibility of using Kiellman paper drains was to be considered as an alternative to sandvicks.

In view of the proposed refinery production programme it was decided that the crude tanks (6 30.70 m diameter by 22 m high) should be pile supported. The reduction in benefit resulting from this is discussed below under Cost Benefit Evaluation of Field Trials. The remaining tankage holding the refined products would consist of either 20 piled tanks, or 34 earth supported tanks, having capacities ranging from 10,000 to 50,000 m³, depending on the results of the embankment load tests.

COST BENEFIT EVALUATION OF FIELD TRIALS

The following cost benefit analysis is based on current tank construction contractors' prices used on similar projects in Europe. The sums quoted, therefore, bear no relationship to the subject project, except insofar as they indicate the magnitude of benefit derived from the engineering studies under discussion.

Regarding steel erection costs, attention is drawn to the old rule: the taller the tank the cheaper it is. This tends to

divide the benefits of constructing an extra set of pilot tanks. However, the sums involved are small compared with the difference in foundation costs, as illustrated in Tables 1 and 2.

Table 1

| Item | Cost (£) | Benefit (£) | Net Cost (£) |
|---------------------------|-----------|-------------|--------------|
| Crude oil | 1,000,000 | 100,000 | 900,000 |
| Programme Project 100,000 | 1,000,000 | 100,000 | 900,000 |
| Programme Project 200,000 | 1,000,000 | 100,000 | 900,000 |

Notes: 1. The tanks 21.5 m high, with support.
2. Heavy tanks 21.5 m high, with support.
3. The tanks 21.5 m high, with support.
4. Heavy tanks 21.5 m high, with support.
5. The tanks 21.5 m high, with support.
6. Heavy tanks 21.5 m high, with support.

Table 2

| Item | Cost (£) | Benefit (£) | Net Cost (£) |
|---|----------|-------------|--------------|
| 1. All tanks filled | 1,000 | 1,000 | 0 |
| 2. All tanks with support | 1,000 | 1,000 | 0 |
| 3. All tanks with support on ground treatment | 1,000 | 1,000 | 0 |
| 4. Tanks filled/empty | 1,000 | 1,000 | 0 |
| 5. Tanks filled/empty | 1,000 | 1,000 | 0 |
| 6. All tanks with support | 1,000 | 1,000 | 0 |
| 7. Tanks filled/empty | 1,000 | 1,000 | 0 |
| 8. Tanks filled/empty | 1,000 | 1,000 | 0 |

A range of saving from £1,300,000 to £10,000 can be shown by comparing the actual construction cost of various methods of treatment with the all-piled case (Scheme A). However, since the proposed production schedule requires the immediate use of the crude tanks, it was decided that they should be pile supported in any case. This reduces the savings accordingly, and in particular brings the maximum end of the range to £930,000.

Estimated costs of providing these savings are as follows:

1. Test embankment cost including engineering supervision, fill, plant hire, instrumentation and contract labour;

2. Installation of instrumentation and fill from embankments £22,000
3. Installation of instrumentation at tank sites £15,000 (£7,500)
4. Supervision of installation and monitoring of tanks £33,000 (£9,000)
5. Estimated costs of more sophisticated engineering, field and laboratory studies associated with earth supported tank design, over that for pile design analysis £15,000
6. Possible re-levelling costs assuming all 34 tanks need to be re-levelled once (Estimated cost of re-levelling one 50 m diameter tank £5,500) £190,000 (£109,000)

Interest on capital investment in product tank-age for six month non-productive period during water testing programme £137,000 (£88,000)

Total cost: £255,000 (£119,000)

Note: Additional amount assuming crude tanks are also earth supported.

Therefore, assuming the more costly form of ground treatment is chosen (sandvicks) a nominal saving of £5,000 is possible. More likely, however, a Kjellman paper drain system would be adopted saving some £285,000; or in the no ground treatment alternative, £225,000. Similarly it can be estimated that a maximum saving of £742,000 could be achieved if production activities allowed all savings to be earth supported, without ground treatment.

Expense No. 6 above emphasizes the value of careful monitoring and pre-engineering, that is a saving in time during tank loading can realise a substantial saving in finance.

Further saving could be achieved if temporary P.V.C. tank bases were to be utilized during water testing. This possibility is at present being studied.

It should also be noted that for any set of tanks, the total volume of crude and product, if spilled, must be retained within fire walls, having a statutory minimum height. Therefore land costs associated with the tank farm are virtually

constant for a given refinery capacity at a given location regardless of the foundation selection.

SITE CONDITIONS

The site of the proposed refinery is situated in relatively flat farmland, protected from flooding by dykes along its southern boundary. The surface elevations at the site range from 0.5 m to 2 m O.D. The sea protection dyke at present has a crest elevation of 6 to 7 m O.D., but is to be heightened to in excess of 7 m, as part of the Thames flood protection scheme. The site is drained by a large number of natural and excavated channels which discharge via tide gates into the Thames.

The test site was chosen on uniform soft soil strata of typical thickness and close to a plentiful and inexpensive source of fill. The subsurface conditions of the test site were investigated by sampling soil from test pits, boreholes (including one 110 mm diameter borehole for 214 mm piston sampling), Delft continuous sampling, Dutch Deep Soundings and in-situ vane testing. Constant head field permeability tests (Gibson 1963, 1966 and 1970 and Wilkinson 1968) were also performed at the site.

In general, Table 3 summarizes the subsurface conditions.

Fig 1 shows the soil state below embankment No. 1

| Soil Type | Description | Depth (m) | Saturated Unit Weight | |
|-------------------------------|--|-----------|-------------------------------------|--------------------------------------|
| | | | γ_{sat} (kN/m ³) | γ_{sat} (lb/ft ³) |
| Heavy clay | Thick, soft to stiff, slightly compressible | 0 | 1.8 - 2.0 | 1.1 - 1.2 |
| Very clayey clay, silty | Soft, very compressible | 1 | 1.6 - 1.8 | 1.0 |
| Very fine sand, silty | Medium dense, stiff, slightly to moderately compressible | 2 | 1.9 - 2.0 | 1.2 - 1.3 |
| Clay and sandy clay | Medium stiff, slightly compressible | 3 | 1.9 | 1.2 - 1.3 |
| Heavy gravel (Thames ballast) | Dense, impermeable | 17 | 2.0 - 2.2 | 1.3 - 1.4 |
| London Clay | Very stiff, very slightly compressible | 24 | | 1.4 - 1.5 |

FIELD AND LABORATORY TESTING

The following tests were performed on the soft soil strata:

1. Consolidation tests on samples 75 mm diameter, 19 mm thick.
2. 254 mm diameter consolidation tests.
3. Consolidated undrained triaxial compression tests with pore pressure measurement on samples, 61 mm diameter, 113 mm high.
4. In-situ constant head permeability tests.

Computed permeabilities from the 254 mm laboratory consolidation tests are shown to be in the range 2.5×10^{-8} to 1.4×10^{-8} cm per second for vertical permeability and 1.5×10^{-8} to 1.6×10^{-8} cm per second for horizontal permeability. Field permeability tests gave a range of 2.0×10^{-8} to 1.2×10^{-8} cm per second.

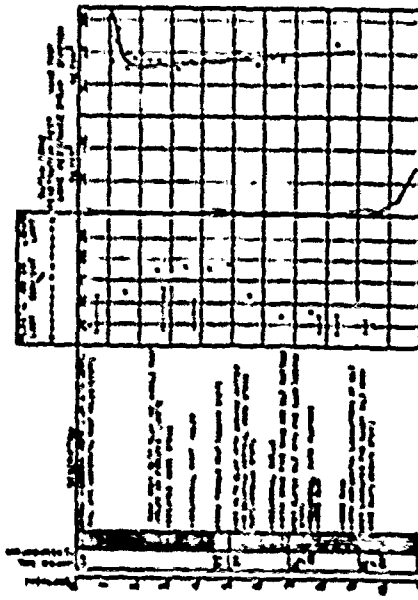


Fig 1 Subsurface conditions, Embankment No. 1

SITE PREPARATION AND FILLING

The proposal to construct the embankment load test was approved by mid-February 1972. Although cost estimates for instrumentation and filling had already been obtained, installation did not proceed until late March. Instrument installation was completed at embankment site No. 1 on 22nd April, where filling proceeded.

The sandwick treatment of embankment site No. 2 was carried out between 17th April and 1st May and the remaining instrumentation was completed by 1st May ready to begin filling on 8th May. This indicates the minimum time for

preparing such a programme.

INSTRUMENTATION - TEST ENSEMBLEMENT

Most of the instrumentation under each embankment was positioned in order to compare directly an instrument associated with one embankment with its duplicate below the other. Table 4 lists instruments installed beneath each embankment, and an average cost in the ground for one instrument or measurement point. The cost includes instruments and materials, and subcontractor charges and technical supervision involved in installation.

| INSTRUMENT | TABLE 4 NUMBER OF INSTRUMENTS PER ENSEMBLEMENT | | | | TOTAL INSTRUMENTS PER ENSEMBLEMENT |
|---|--|-------|-------|-------|---------------------------------------|
| | NO. 1 | NO. 2 | NO. 3 | NO. 4 | |
| Piezometer | 10 | 5 | 10 | | 25 |
| Hydraulic settlement gauge points | 4 | 3 | 7 | | 14 |
| Borehole settlement gauge points | 11 | | 11 | | 22 |
| Mole settlement gauge points | 3 | 3 | 6 | | 12 |
| Settlement access holes | 4 | 2 | 7 | | 13 |
| Survey markers | 10 | 10 | 20 | | 40 |
| Notes: Relating to (1) to full monitoring programme, e.g. for mole settlement access holes, the per cent of profile relating to 1/10 in full monitoring programme. | | | | | 0.75 |

Fig 2 below shows the location of each of the instruments.

- The individual instruments are indicated as follows:
- Initial figure indicates embankment number
 - Letters indicate type of instrument as follows:
 - P - piezometer, I - inclinometer, M - hydraulic settlement gauge, B - borehole settlement gauge
 - Last figure indicates number of particular instrument or measurement point, e.g. 127 indicates piezometer No. 7 in embankment No. 1.

Settlement measurement
Three independent systems of measuring settlement beneath the embankment were used. The hydraulic settlement gauges and the mole settlement profiling system were installed so that a comparison could be made between two methods of remote settlement measurement, which might be used beneath tackle. The borehole settlement gauge was included to give settlement of individual layers of strata. A comparative plot of settlement versus time below the centre of the tanks for the three methods of measurement is shown in Fig 4. Sensibly

identical results were given by the hydraulic gauge and the surface borehole settlement gauge, the mole gave somewhat higher settlements.

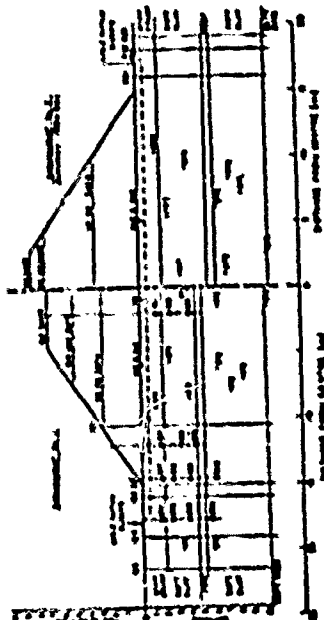


Fig 2 Location of instruments below each embankment

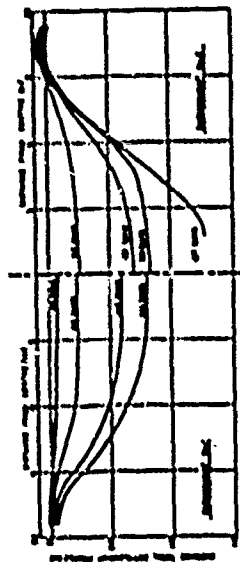


Fig 3 Typical settlement profiles derived from mole

Fig 4 Settlement Fig 4 A modified version of the Building Research Station pattern overflow type was used. The modification was necessary since the gauge house installation was located at a level above the cell weir, making it necessary to apply a partial vacuum to the ends of the stand pipe to raise the equilibrium level. Despite the agreement in Fig 4, this method proved generally to be unreliable insofar as readings were difficult to repeat and it appeared to be susceptible to operator factors. Moreover, operation was tedious and time-consuming.

Provision and installation costs associated with this system were high and even had the system functioned reliably it is

doubtful that it would have been used for tank water testing.

Mole Settlement Gauge. The mole settlement gauge was potentially the most useful item of instrumentation included in the embankment load test, as it can give a complete profile of settlement immediately beneath a loaded area. This is particularly important when considering its application in storage tank loading programs, where tank bottom shape is of critical importance; it is normally oversteers of base plates, which heralds tank failure. Moreover, it has only been possible to measure settlement of tank shells, and isolated points below tanks using systems such as the hydraulic or mercury settlement gauges. Profiling of the base plates can normally be achieved only by leveling within an empty tank, or by using diver inspection during water testing.

The basic design of the mole is due to Bergdahl and Brown (1967) and a primitive version was manufactured by the writers for tank loading tests at Glibury (Parry 1973).

The commercially manufactured system used in the present tests consists of a flexible access tube, which is placed in a trench below the loaded area, and a probe (the mole) which is inserted into the access tube. The instrument measures settlement at any number of points across the profile, relative to a concrete datum block. The probe contains a bladder connected to an electrical transducer by a nylon tube filled with liquid (water). The transducer is located in a recorder box which rests on the datum block. Change in negative pressure in the transducer is converted to an electrical signal, and is indicated on a direct reading meter as a difference in elevation between datum and probe.

Three flexible access tubes disposed at equal horizontal angles were placed under each embankment in the base of sand-filled trenches approximately 0.6 m deep. The tubes crossed at the centre and were concreted at both ends into 0.5 m square 0.3 m thick datum pads. It can be seen in Fig 1 that settlements recorded by the mole were larger than recorded by the other two measuring devices.

It was found that small fluctuations in temperature caused the system to give errors of up to 70 percent during the early stages of loading, when the settlements were less than 0.2 m. It was necessary to lay the tube out on the ground before insertion, exposing it to atmospheric conditions. It proved to be very sensitive to the sun's heat, and to reduce errors, a policy of night time operation was adopted. An obvious improvement would be to use a probe fluid with a smaller coefficient of expansion.

Mole readings could be obtained from all access tubes below

embankment No. 2 until the slip occurred. After the slip, one of the access tubes which passed through the slip zone kicked up 0.3 m above ground level, in the heavy zone between the toe of the bank and the datum block. From the other end it could only be penetrated 19 m to the centre of the bank. Another tube passing through the slip zone could be penetrated for a distance of 1 m from the heavy zone end, and 20 m from the other end. The datum block in the heavy zone in this case moved out radially by about 50 mm. The third access tube, which appeared not to pass through the slip zone, could be probed 19 m from either end to the centre of the bank, but not beyond this point. The entire settlement at this time was about 1.25 m.

Even so, the system has continued to give further information with respect to the continuous settlement of the embankment, while all other methods have failed. Fig 3 shows typical settlement profiles derived from use of the mole for both embankments, and can be compared with full loads shown in Fig 2.

Borehole Settlement Gauge. The system is described by Bergdahl and Smith (1971) and consists of magnetic rings set in a borehole at the levels where settlements are to be measured. The magnetic rings were set in short lengths of rigid PVC cylinder which were spring-loaded against the side of the borehole and surrounded a central PVC access tube. A probe containing reed switches was lowered down the access tube to determine the depth of each magnetic ring. An audible signal indicates reed switch activation. The borehole was backfilled with cement/bentonite grout after placing the units.

This equipment was installed only below embankment No. 1 to obtain additional information regarding settlement of various strata; its design would obviously prohibit its use beneath tank foundations.

This system of settlement measurement was certainly the simplest and quickest to operate and potentially the most accurate of the three. However, the design of the system adopted was not considered ideal for the soft clay conditions.

Problems encountered were:

- a) When settlements at the surface reached about 2.5 m, the large movements and downward of the fill caused the PVC access tube to distort, preventing probe entry. Thus the readings for the instruments shown in Fig 4 terminated before the fill had reached full height, and
- b) Certain of the spring PVC magnetic ring units

appeared to jam against the probe access tube, and slip relative to the soft sides of the borehole.

These limitations might be overcome by using telescopic access tube and magnetic units with mechanical anchors, which penetrate further into the borehole wall.

Pore Water Pressure Measurement - Piezometers
All piezometers were of the type described by Wilkes (1970); basically a simple Casagrande piezometer tip welded to be pushed into soft and loose soils at the base of a borehole. A few of the piezometers (1P1, 1P4, 1P6 and 1P8) were placed in sand cells at the bottom of boreholes. All boreholes were sealed with bentonite/cement grout. The piezometers were each connected to a double line mercury manometer pressure measurement system. All piezometers were installed below the water table.

The in-situ constant head permeability tests referred to above were performed at three piezometers installed midway between the two embankments at depths of 3.4, 5.0 and 7.0 m.

It was found that the system required frequent de-airing, in particular during the early stages of loading, when piezometric levels were below the header tank level, which established at 3.32 m O.D. However, once the pore pressures had increased to a level corresponding to the header tank, little or no de-airing was necessary. Prior to this pressure being attained, de-airing was necessary after about every tenth reading.

A general rule regarding the need for de-airing was enforced such that: i) manometers were de-aired if air bubbles could be detected visually; and ii) piezometers were de-aired if the difference between the two manometer readings was in excess of 10 mm.

Fig 4 above changes in pore pressure at 1P1, 1P2, 2P1, 2P2, and also height of fill, both plotted against time in days. Plots of excess pore pressure against fill height are shown in Fig 5.

The ground pressure is not a linear function of fill height, because the amount of fill placed per unit of height decreases. The ratio du/dz of excess pore pressure to increase in major principal stress (from elastic stress distribution) of these piezometer tips for fill heights of 3 m and 6 m is given below:

| Piezometer | 1P1 | 1P2 | 2P1 | 2P2 |
|--------------------|-----|-----|-----|-----|
| Fill Height (m) | 3 | 6 | 3 | 6 |
| du/dσ _v | .60 | .83 | .16 | .75 |
| | | | .62 | 1.0 |
| | | | | .16 |
| | | | | .73 |

It can be seen that the ratio du/dσ_v increases with fill height as expected for a lightly overconsolidated clay.

The piezometer system was simple to operate but time consuming and appeared to give consistent and reliable data.

The large strains associated with the slip in embankment No. 2 broke the piezometer leads and put them out of action. The maximum settlement at this time was 1.0 m. Fig 5 shows that no clear indication of the imminent slip in embankment No. 2 was recorded by the piezometer system.

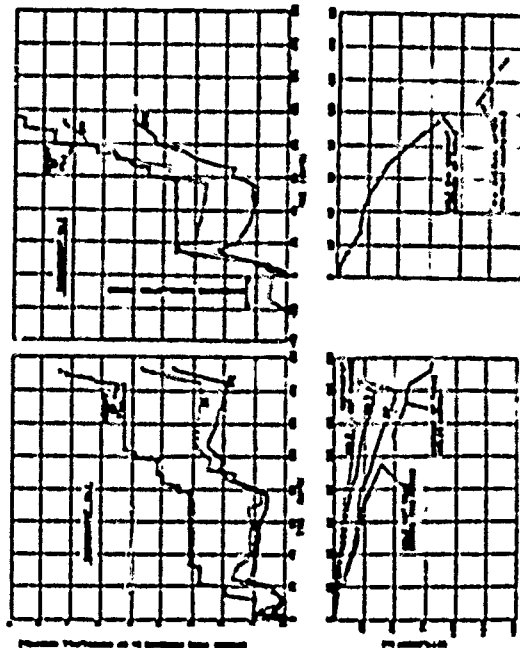
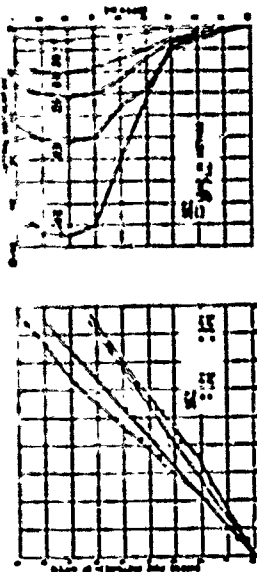


Fig 4 Pore Pressure, Settlement and Excess Pore Pressure versus Time

Lateral Earth Deformation Measurement - Incliner-meter
A potentiometer type inclinometer with digital direct reading unit was employed to measure the lateral deformation of substrata. The torpedo was 0.7 m in overall length and ran on four keyways inside 30 mm internal diameter aluminium access tube, grouted into 0.15 m diameter boreholes. The results from this instrument were considered adequate and its operation straightforward, but there were periods when the instrument was out of operation due to faults, arising in some measure from operator inexperience.

1. The first step in the process of the investigation is the identification of the problem. This is done by the investigator who is assigned to the case. The investigator will then gather information about the problem and the people involved. This information will be used to develop a plan of action.



**Fig 5 Excess pore pressure
versus sill height**

Instrument Reading and Reduction Times

Table 5 indicates the time required by a technician for data collection and reduction for each instrument. Reduction times are based on hand methods; computerization would reduce them by 70 percent.

| DATE | TIME | LOCATION | NO. OF BIRDS | NO. OF EGGS | NO. OF CHICKS | NO. OF ADULTS | NO. OF YOUNG |
|--------|-------|--------------------------|--------------|-------------|---------------|---------------|--------------|
| 1940 | 10:30 | 1000 ft. above sea level | 10 | 10 | 10 | 10 | 10 |
| 1940 | 11:00 | 1000 ft. above sea level | 10 | 10 | 10 | 10 | 10 |
| 1940 | 11:30 | 1000 ft. above sea level | 10 | 10 | 10 | 10 | 10 |
| 1940 | 12:00 | 1000 ft. above sea level | 10 | 10 | 10 | 10 | 10 |
| 1940 | 12:30 | 1000 ft. above sea level | 10 | 10 | 10 | 10 | 10 |
| 1940 | 13:00 | 1000 ft. above sea level | 10 | 10 | 10 | 10 | 10 |
| 1940 | 13:30 | 1000 ft. above sea level | 10 | 10 | 10 | 10 | 10 |
| 1940 | 14:00 | 1000 ft. above sea level | 10 | 10 | 10 | 10 | 10 |
| 1940 | 14:30 | 1000 ft. above sea level | 10 | 10 | 10 | 10 | 10 |
| 1940 | 15:00 | 1000 ft. above sea level | 10 | 10 | 10 | 10 | 10 |
| 1940 | 15:30 | 1000 ft. above sea level | 10 | 10 | 10 | 10 | 10 |
| 1940 | 16:00 | 1000 ft. above sea level | 10 | 10 | 10 | 10 | 10 |
| 1940 | 16:30 | 1000 ft. above sea level | 10 | 10 | 10 | 10 | 10 |
| 1940 | 17:00 | 1000 ft. above sea level | 10 | 10 | 10 | 10 | 10 |
| 1940 | 17:30 | 1000 ft. above sea level | 10 | 10 | 10 | 10 | 10 |
| 1940 | 18:00 | 1000 ft. above sea level | 10 | 10 | 10 | 10 | 10 |
| 1940 | 18:30 | 1000 ft. above sea level | 10 | 10 | 10 | 10 | 10 |
| 1940 | 19:00 | 1000 ft. above sea level | 10 | 10 | 10 | 10 | 10 |
| 1940 | 19:30 | 1000 ft. above sea level | 10 | 10 | 10 | 10 | 10 |
| 1940 | 20:00 | 1000 ft. above sea level | 10 | 10 | 10 | 10 | 10 |
| 1940 | 20:30 | 1000 ft. above sea level | 10 | 10 | 10 | 10 | 10 |
| 1940 | 21:00 | 1000 ft. above sea level | 10 | 10 | 10 | 10 | 10 |
| 1940 | 21:30 | 1000 ft. above sea level | 10 | 10 | 10 | 10 | 10 |
| 1940 | 22:00 | 1000 ft. above sea level | 10 | 10 | 10 | 10 | 10 |
| 1940 | 22:30 | 1000 ft. above sea level | 10 | 10 | 10 | 10 | 10 |
| 1940 | 23:00 | 1000 ft. above sea level | 10 | 10 | 10 | 10 | 10 |
| 1940 | 23:30 | 1000 ft. above sea level | 10 | 10 | 10 | 10 | 10 |
| 1940 | 24:00 | 1000 ft. above sea level | 10 | 10 | 10 | 10 | 10 |
| 1940 | 24:30 | 1000 ft. above sea level | 10 | 10 | 10 | 10 | 10 |
| 1940 | 25:00 | 1000 ft. above sea level | 10 | 10 | 10 | 10 | 10 |
| 1940 | 25:30 | 1000 ft. above sea level | 10 | 10 | 10 | 10 | 10 |
| 1940 | 26:00 | 1000 ft. above sea level | 10 | 10 | 10 | 10 | 10 |
| 1940 | 26:30 | 1000 ft. above sea level | 10 | 10 | 10 | 10 | 10 |
| 1940 | 27:00 | 1000 ft. above sea level | 10 | 10 | 10 | 10 | 10 |
| 1940 | 27:30 | 1000 ft. above sea level | 10 | 10 | 10 | 10 | 10 |
| 1940 | 28:00 | 1000 ft. above sea level | 10 | 10 | 10 | 10 | 10 |
| 1940 | 28:30 | 1000 ft. above sea level | 10 | 10 | 10 | 10 | 10 |
| 1940 | 29:00 | 1000 ft. above sea level | 10 | 10 | 10 | 10 | 10 |
| 1940 | 29:30 | 1000 ft. above sea level | 10 | 10 | 10 | 10 | 10 |
| 1940 | 30:00 | 1000 ft. above sea level | 10 | 10 | 10 | 10 | 10 |
| 1940 | 30:30 | 1000 ft. above sea level | 10 | 10 | 10 | 10 | 10 |
| 1940 | 31:00 | 1000 ft. above sea level | 10 | 10 | 10 | 10 | 10 |
| 1940 | 31:30 | 1000 ft. above sea level | 10 | 10 | 10 | 10 | 10 |
| 1940 | 32:00 | 1000 ft. above sea level | 10 | 10 | 10 | 10 | 10 |
| 1940 | 32:30 | 1000 ft. above sea level | 10 | 10 | 10 | 10 | 10 |
| 1940 | 33:00 | 1000 ft. above sea level | 10 | 10 | 10 | 10 | 10 |
| 1940 | 33:30 | 1000 ft. above sea level | 10 | 10 | 10 | 10 | 10 |
| 1940 | 34:00 | 1000 ft. above sea level | 10 | 10 | 10 | 10 | 10 |
| 1940 | 34:30 | 1000 ft. above sea level | 10 | 10 | 10 | 10 | 10 |
| 1940 | 35:00 | 1000 ft. above sea level | 10 | 10 | 10 | 10 | 10 |
| 1940 | 35:30 | 1000 ft. above sea level | 10 | 10 | 10 | 10 | 10 |
| 1940 | 36:00 | 1000 ft. above sea level | 10 | 10 | 10 | 10 | 10 |
| 1940 | 36:30 | 1000 ft. above sea level | 10 | 10 | 10 | 10 | 10 |
| 1940 | 37:00 | 1000 ft. above sea level | 10 | 10 | 10 | 10 | 10 |
| 1940 | 37:30 | 1000 ft. above sea level | 10 | 10 | 10 | 10 | 10 |
| 1940 | 38:00 | 1000 ft. above sea level | 10 | 10 | 10 | 10 | 10 |
| 1940 | 38:30 | 1000 ft. above sea level | 10 | 10 | 10 | 10 | 10 |
| 1940 | 39:00 | 1000 ft. above sea level | 10 | 10 | 10 | 10 | 10 |
| 1940 | 39:30 | 1000 ft. above sea level | 10 | 10 | 10 | 10 | 10 |
| 1940 | 40:00 | 1000 ft. above sea level | 10 | 10 | 10 | 10 | 10 |
| 1940 | 40:30 | 1000 ft. above sea level | 10 | 10 | 10 | 10 | 10 |
| 1940 | 41:00 | 1000 ft. above sea level | 10 | 10 | 10 | 10 | 10 |
| 1940 | 41:30 | 1000 ft. above sea level | 10 | 10 | 10 | 10 | 10 |
| 1940 | 42:00 | 1000 ft. above sea level | 10 | 10 | 10 | 10 | 10 |
| 1940 | 42:30 | 1000 ft. above sea level | 10 | 10 | 10 | 10 | 10 |
| 1940 | 43:00 | 1000 ft. above sea level | 10 | 10 | 10 | 10 | 10 |
| 1940 | 43:30 | 1000 ft. above sea level | 10 | 10 | 10 | 10 | 10 |
| 1940 | 44:00 | 1000 ft. above sea level | 10 | 10 | 10 | 10 | 10 |
| 1940 | 44:30 | 1000 ft. above sea level | 10 | 10 | 10 | 10 | 10 |
| 1940 | 45:00 | 1000 ft. above sea level | 10 | 10 | 10 | 10 | 10 |
| 1940 | 45:30 | 1000 ft. above sea level | 10 | 10 | 10 | 10 | 10 |
| 1940 | 46:00 | 1000 ft. above sea level | 10 | 10 | 10 | 10 | 10 |
| 1940 | 46:30 | 1000 ft. above sea level | 10 | 10 | 10 | 10 | 10 |
| 1940 | 47:00 | 1000 ft. above sea level | 10 | 10 | 10 | 10 | 10 |
| 1940 | 47:30 | 1000 ft. above sea level | 10 | 10 | 10 | 10 | 10 |
| 1940 | 48:00 | 1000 ft. above sea level | 10 | 10 | 10 | 10 | 10 |
| 1940 | 48:30 | 1000 ft. above sea level | 10 | 10 | 10 | 10 | 10 |
| 1940 | 49:00 | 1000 ft. above sea level | 10 | 10 | 10 | 10 | 10 |
| 1940 | 49:30 | 1000 ft. above sea level | 10 | 10 | 10 | 10 | 10 |
| 1940 | 50:00 | 1000 ft. above sea level | 10 | 10 | 10 | 10 | 10 |
| 1940 | 50:30 | 1000 ft. above sea level | 10 | 10 | 10 | 10 | 10 |
| 1940 | 51:00 | 1000 ft. above sea level | 10 | 10 | 10 | 10 | 10 |
| 1940 | 51:30 | 1000 ft. above sea level | 10 | 10 | 10 | 10 | 10 |
| 1940 | 52:00 | 1000 ft. above sea level | 10 | 10 | 10 | 10 | 10 |
| 1940 | 52:30 | 1000 ft. above sea level | 10 | 10 | 10 | 10 | 10 |
| 1940 | 53:00 | 1000 ft. above sea level | 10 | 10 | 10 | 10 | 10 |
| 1940 | 53:30 | 1000 ft. above sea level | 10 | 10 | 10 | 10 | 10 |
| 1940 | 54:00 | 1000 ft. above sea level | 10 | 10 | 10 | 10 | 10 |
| 1940 | 54:30 | 1000 ft. above sea level | 10 | 10 | 10 | 10 | 10 |
| 1940 | 55:00 | 1000 ft. above sea level | 10 | 10 | 10 | 10 | 10 |
| 1940 | 55:30 | 1000 ft. above sea level | 10 | 10 | 10 | 10 | 10 |
| 1940 | 56:00 | 1000 ft. above sea level | 10 | 10 | 10 | 10 | 10 |
| 1940 | 56:30 | 1000 ft. above sea level | 10 | 10 | 10 | 10 | 10 |
| 1940 | 57:00 | 1000 ft. above sea level | 10 | 10 | 10 | 10 | 10 |
| 1940 | 57:30 | 1000 ft. above sea level | 10 | 10 | 10 | 10 | 10 |
| 1940 | 58:00 | 1000 ft. above sea level | 10 | 10 | 10 | 10 | 10 |
| 1940 | 58:30 | 1000 ft. above sea level | 10 | 10 | 10 | 10 | 10 |
| 1940 | 59:00 | 1000 ft. above sea level | 10 | 10 | 10 | 10 | 10 |
| 1940 | 59:30 | 1000 ft. above sea level | 10 | 10 | 10 | 10 | 10 |
| 1940 | 60:00 | 1000 ft. above sea level | 10 | 10 | 10 | 10 | 10 |
| 1940 | 60:30 | 1000 ft. above sea level | 10 | 10 | 10 | 10 | 10 |
| 1940 | 61:00 | 1000 ft. above sea level | 10 | 10 | 10 | 10 | 10 |
| 1940 | 61:30 | 1000 ft. above sea level | 10 | 10 | 10 | 10 | 10 |
| 1940 | 62:00 | 1000 ft. above sea level | 10 | 10 | 10 | 10 | 10 |
| 1940 | 62:30 | 1000 ft. above sea level | 10 | 10 | 10 | 10 | 10 |
| 1940 | 63:00 | 1000 ft. above sea level | 10 | 10 | 10 | 10 | 10 |
| 1940 | 63:30 | 1000 ft. above sea level | 10 | 10 | 10 | 10 | 10 |
| 1940 | 64:00 | 1000 ft. above sea level | 10 | 10 | 10 | 10 | 10 |
| 1940 | 64:30 | 1000 ft. above sea level | 10 | 10 | 10 | 10 | 10 |
| 1940 | 65:00 | 1000 ft. above sea level | 10 | 10 | 10 | 10 | 10 |
| 1940 | 65:30 | 1000 ft. above sea level | 10 | 10 | 10 | 10 | 10 |
| 1940 | 66:00 | 1000 ft. above sea level | 10 | 10 | 10 | 10 | 10 |
| 1940 | 66:30 | 1000 ft. above sea level | 10 | 10 | 10 | 10 | 10 |
| 1940 | 67:00 | 1000 ft. above sea level | 10 | 10 | 10 | 10 | 10 |
| 1940 | 67:30 | 1000 ft. above sea level | 10 | 10 | 10 | 10 | 10 |
| 1940 | 68:00 | 1000 ft. above sea level | 10 | 10 | 10 | 10 | 10 |
| 1940 | 68:30 | 1000 ft. above sea level | 10 | 10 | 10 | 10 | 10 |
| 1940 | 69:00 | 1000 ft. above sea level | 10 | 10 | 10 | 10 | 10 |
| 1940 | 69:30 | 1000 ft. above sea level | 10 | 10 | 10 | 10 | 10 |
| 1940 | 70:00 | 1000 ft. above sea level | 10 | 10 | 10 | 10 | 10 |
| 1940 | 70:30 | 1000 ft. above sea level | 10 | 10 | 10 | 10 | 10 |
| 1940 | 71:00 | 1000 ft. above sea level | 10 | 10 | 10 | 10 | 10 |
| 1940 | 71:30 | 1000 ft. above sea level | 10 | 10 | 10 | 10 | 10 |
| 1940 | 72:00 | 1000 ft. above sea level | 10 | 10 | 10 | 10 | 10 |
| 1940 | 72:30 | 1000 ft. above sea level | 10 | 10 | 10 | 10 | 10 |
| 1940 | 73:00 | 1000 ft. above sea level | 10 | 10 | 10 | 10 | 10 |
| 1940 | 73:30 | 1000 ft. above sea level | 10 | 10 | 10 | 10 | 10 |
| 1940 | 74:00 | 1000 ft. above sea level | 10 | 10 | 10 | 10 | 10 |
| 1940 | 74:30 | 1000 ft. above sea level | 10 | 10 | 10 | 10 | 10 |
| 1940 | 75:00 | 1000 ft. above sea level | 10 | 10 | 10 | 10 | 10 |
| 1940 | 75:30 | 1000 ft. above sea level | 10 | 10 | 10 | 10 | 10 |
| 1940 | 76:00 | 1000 ft. above sea level | 10 | 10 | 10 | 10 | 10 |
| 1940 | 76:30 | 1000 ft. above sea level | 10 | 10 | 10 | 10 | 10 |
| 1940 | 77:00 | 1000 ft. above sea level | 10 | 10 | 10 | 10 | 10 |
| 1940 | 77:30 | 1000 ft. above sea level | 10 | 10 | 10 | 10 | 10 |
| 1940 | 78:00 | 1000 ft. above sea level | 10 | 10 | 10 | 10 | 10 |
| 1940 | 78:30 | 1000 ft. above sea level | 10 | 10 | 10 | 10 | 10 |
| 1940 | 79:00 | 1000 ft. above sea level | 10 | 10 | 10 | 10 | 10 |
| 1940 | 79:30 | 1000 ft. above sea level | 10 | 10 | 10 | 10 | 10 |
| 1940 | 80:00 | 1000 ft. above sea level | 10 | 10 | 10 | 10 | 10 |
| 1940 | 80:30 | 1000 ft. above sea level | 10 | 10 | 10 | 10 | 10 |
| 1940 | 81:00 | 1000 ft. above sea level | 10 | 10 | 10 | 10 | 10 |
| 1940 | 81:30 | 1000 ft. above sea level | 10 | 10 | 10 | 10 | 10 |
| 1940 | 82:00 | 1000 ft. above sea level | 10 | 10 | 10 | 10 | 10 |
| 1940 | 82:30 | 1000 ft. above sea level | 10 | 10 | 10 | 10 | 10 |
| 1940 | 83:00 | 1000 ft. above sea level | 10 | 10 | 10 | 10 | 10 |
| 1940 | 83:30 | 1000 ft. above sea level | 10 | 10 | 10 | 10 | 10 |
| 1940 | 84:00 | 1000 ft. above sea level | 10 | 10 | 10 | 10 | 10 |
| 1940</ | | | | | | | |

DISSEMINATE YOUR VOTING MESSAGE

It is proposed that the earth supported loads will be monitored using the following instrumentation scheme:

- (25) All tanks to have shell settlement tags welded at eight points around the circumference:

- At least two tanks to be instrumented with eight transmitters.

History

The commercial instrumentation used for the trial loading tests has, in general, proved satisfactory in producing results of the required accuracy. A particular advantage of the Campbell test has been the opportunity to experiment with various systems, particularly automatic measurements, to be made on suitable instruments and location of instruments, to be chosen for monitoring tanks. As a result of these trials one instrument originally intended to be used for this purpose has been found to be either unnecessary or unsuitable and the trials have consequently led to a saving of time and money.

CONCLUSIONS

The study reported here was commissioned by Occidental Insurance Co. The direction of Mr. R. M. Stubbings of that firm is especially acknowledged.

THE UNIVERSITY OF CHICAGO

- Bergdahl, U. and Broms, B.B. (1967) New methods of measuring in-situ settlements. *Journal of S.M. A.S.T.M.*
- Berland, J.B., Moore, J.P.A. and Smith, P.T.K. (1972) A simple and precise borehole extensometer. *Geotechnique* Vol. 22 No. 1.
- Dashtidar, A.S., Gupta, S. (1967) Application of sandvics in housing project. *Seventh International Conference of the International Society of Soil Mechanics and Foundation Engineering, Mexico.*
- Gibson, R.E. (1963) An analysis of system flexibility and its effect on time-lag in pore water pressure measurement. Vol. 13 No. 1.
- Gibson, R. (1966) A note on the constant head tests to measure soil permeability in-situ. *Geotechnique* Vol. 16 No. 3.
- Gibson, R.E. (1972) An extension to the theory of the constant head permeability test. *Geotechnique* Vol. 22 No. 2.
- Parry, R.M.C. (1970) Discussion In-situ Investigation in Soils and Rock Conference Proceedings. *British Geotechnical Society.*
- Waters, P.T. (1970) A note on the installation of piezometers in small diameter boreholes. *Geotechnique* Vol. 20 No. 3.
- Williamson, V.B. (1966) Constant head in-situ permeability tests in clay strata. *Geotechnique* Vol. 18 No. 2.

The Response of a Soft Clay Layer to Embankment Loading

by

M. J. PENDER, B.E. (Hons), Ph.D., M.N.Z.I.E.
Geomechanics Engineer, Ministry of Works & Development, N.Z.

R. H. G. PARRY, M.A., Ph.D., M.I.E.Aust
Lecturer, University of Cambridge, England

and

P. J. GEORGE, B.Sc.
Engineer, Lloyds Register of Shipping, formerly with Dames & Moore, London, U.K.

SUMMARY. The pore pressure response of a soft clay layer subjected to embankment loading is interpreted. Good qualitative agreement is found between the observed pore pressures and those expected on the basis that a lightly overconsolidated clay will exhibit a well defined yield locus. This concept leads to the prediction of a three-part response corresponding to elastic behaviour, yielding, and contained failure. The observed pore pressures were compared with total stresses calculated by a non-linear elastic finite element analysis.

1 INTRODUCTION

At Canvey Island in Essex a major U.K. oil refinery is to be constructed at a site adjacent to the mouth of the River Thames. This paper describes some aspects of the interpretation of the behaviour of one of two small trial embankments constructed as part of the site investigation.

In particular it was desired to examine the observed pore pressure response in terms of some modern ideas about the behaviour of soft clay. Critical state soil mechanics provides a consistent set of concepts relevant to the stress-strain behaviour and pore pressure response of soil, Schofield and Wroth (Ref. 1). These make it possible to predict the general features of the immediate pore pressure response in a field loading situation. The qualitative validity of this prediction is investigated here.

The pore pressure behaviour was measured with hydraulic piezometers installed at several positions beneath the embankment. These observed pressures were related to the calculated changes in vertical stress at the piezometer locations. This stress distribution was determined with a finite element program capable of performing non-linear elastic analysis. Much of the input data for the computer runs was obtained from in-situ tests with the Cankometer, as described in a companion paper (Ref. 2).

Foundations for the product tanks at the refinery could be either pile or earth supported. As there were clear economic benefits for the alternative without piles two trial embankments were constructed to simulate the tank load. These were circular with 30 m base diameter and 1:1 side slopes, and constructed from compacted granular fill. A more detailed description of the site and instrument details is given by George and Parry (Ref. 3), along with a useful discussion of the economics of such an investigation and comments on the performance of the various instruments.

2 BACKGROUND

A central feature of the present interpretation is the concept that a lightly overconsolidated clay will exhibit a yield locus. Because of the overconsolidation the in-situ stress state will be within the locus and hence, initially, the soil will

show an elastic response to additional loading. The locus represents the boundary of all the stress states for which the soil is assumed to behave elastically. As such it represents a generalisation of the preconsolidation concept.

After the stress path engages the yield locus, plastic strain becomes dominant and the pore pressure response much more significant. As the stress path moves outward the soil work hardens and the yield locus is expanded. These ideas are illustrated in Fig. 1.

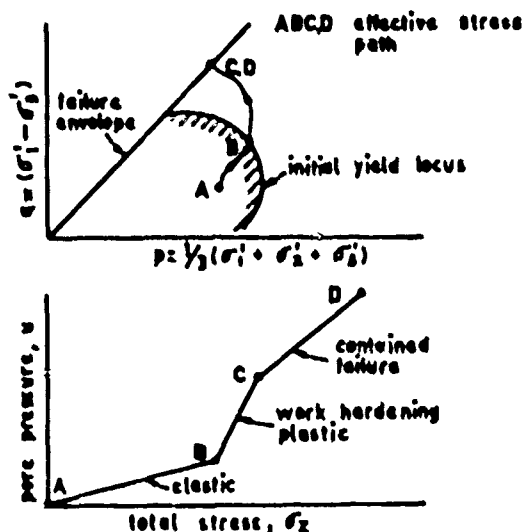


Fig. 1 Yield locus and pore pressure response

The yield locus concept leads to the suggestion that the pore pressure response of a lightly overconsolidated clay under field loading will exhibit three distinct phases. Firstly there is an initial elastic response for stress paths within the yield locus. Secondly when the stress path engages the yield locus there should be a fairly sharp steepening in the pore pressure response curve accompanying the plastic deformation. Finally in undrained loading an element of soil may

reach contained failure, so that no further shear stress can be sustained by that particular piece of soil. Thus any additional stress increment must be isotropic and balanced by an equal change in pore pressure. This means that the pore pressure increase during contained failure will be less rapid than that when yielding is occurring. However, Wroth (Ref. 4) has suggested that there may be some soils in which the rate of pore pressure build up for the second stage is the same as that for the final stage, so the second kink in the pore pressure response curve may not always be observed. This might explain why D'Appolonia et al (Ref. 5) and Hoeg et al (Ref. 6) observed a pore pressure response with only one abrupt change in slope.

In interpreting the response a suitable variable must be chosen against which to plot observed pore pressures. It was decided to use the calculated vertical stress induced by the embankment load. This stress component was selected because another study, Hoeg et al (Ref. 7) has found that this stress component is not greatly affected by non-linear material properties (at least for the case of uniform pressure loading). Also the vertical total stress increase has traditionally been used as a gauge of pore pressure response.

3 SITE CONDITIONS AND SOIL PROPERTIES

Fig. 2 gives a brief log of the soil profile along with the Atterberg Limits and in-situ water content. More detailed information is given in Ref. 3. In-situ shear strength, horizontal effective stress and undrained stiffness data, all determined with the Camkometer, are given in a companion paper, Hughes et al (Ref. 2). Beneath the crust there is a uniform increase in strength, horizontal effective stress and undrained stiffness with depth. This trend is not apparently affected by the change in material type at a depth of approximately 6 m.

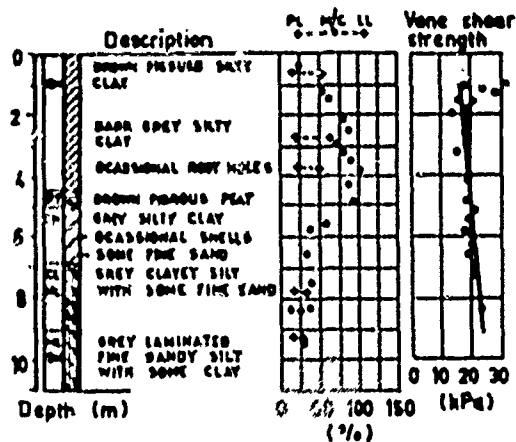


Fig. 2 Subsurface conditions

Dutch penetrometer probings show a very substantial increase in resistance at a depth of 10 m. Thus in the following analysis the soil profile is idealised as a 10 m layer resting on a rough rigid base.

Undisturbed samples, 54 mm in diameter, were taken with a Geonor piston sampler. A number of triaxial specimens, 54 mm in diameter, were prepared from a sample taken between 3 and 4 m depth. These were subjected to stress controlled drained triaxial

tests with different stress paths so that the yield locus might be determined. Yielding was presumed to have occurred when a break was observed in the stress-strain curve. It is of interest to note that the same yield stress was determined with respect to volumetric and distortional strains. Small stress increments were applied and left in place until volume change had almost ceased. For pre-yield load increments this required 1 to 2 days and for post-yield increments 4 to 6 days. The specimens had a height to diameter ratio of unity and lubricated end platens. The cell fluid used was a silicone oil. A back pressure of 200 kPa was applied to ensure saturation. The results of one of the tests and the resulting yield locus are given in Figs. 3 and 4 respectively.

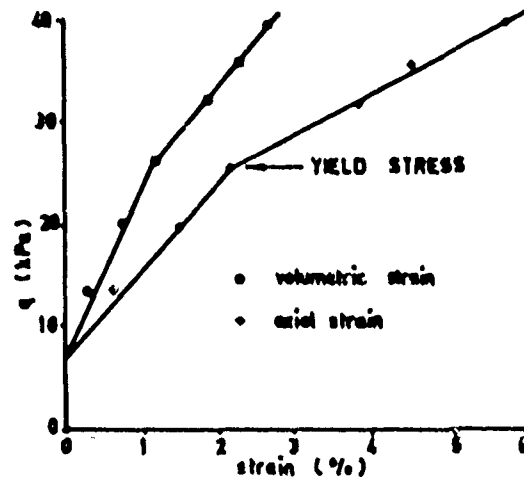


Fig. 3 Result of conventional drained triaxial test

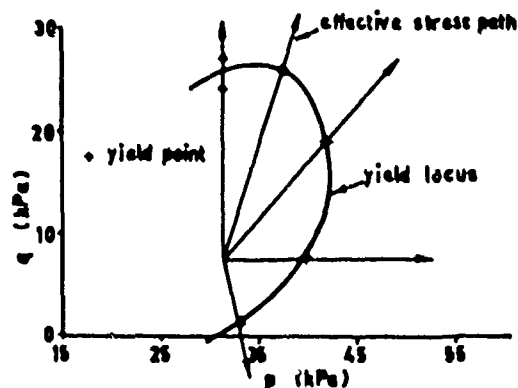


Fig. 4 Yield locus from triaxial tests

4 FIELD RESULTS

The field results from four selected piezometers (at locations indicated in Fig. 6) were examined and the undrained response (i.e. the summation of changes in piezometer readings on the application of load increments) is plotted against embankment height in Fig. 5. It is encouraging to note that this plot suggests three separate phases in the pore pressure response curve.

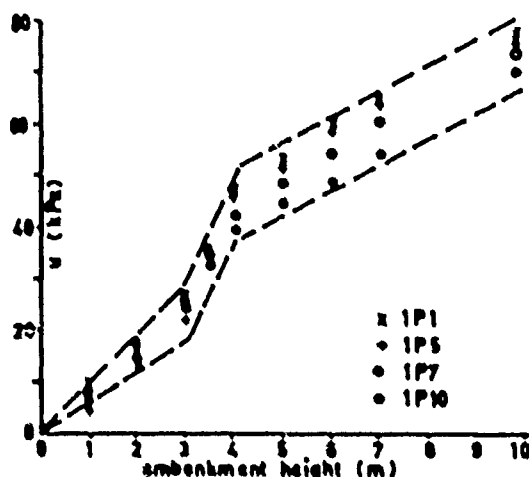


Fig. 5 Observed pore pressures

5 FINITE ELEMENT ANALYSIS

The stresses induced in the soil layer by the construction of the trial embankment were calculated by finite element analysis. The program used was that described by Hollingshead and Raymond (Ref. 8). It performs a non-linear elastic analysis by modifying the element modulus so that a specified stress-strain curve is followed. The data input allows for a variation in Young's modulus with stress, but a constant Poisson's ratio. Any point on the curve is modelled by calculating an equivalent secant modulus. New element moduli are calculated between iterations and the analysis repeated until an acceptable solution is reached. The stress on which the non-linearity is based is the maximum principal stress difference, any effect of the intermediate principal stress is not considered.

The finite element mesh is given in Fig. 6. The locations of the four piezometers of interest are also shown in this diagram. The modelling of the embankment building process was done by manually changing the properties of successive rows of embankment elements between runs of the program. The elements above the current construction level were present in the mesh but were allocated no weight and very small stiffness.

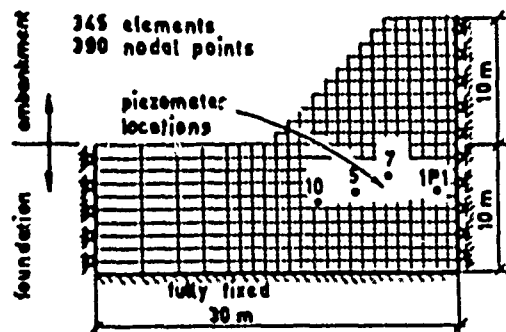


Fig. 6 Finite element mesh

The foundation material was divided into 10 equal layers with different properties, as set out in Table I.

TABLE I

| Material | E (kPa) $\times 10^6$ | ν | γ (kN/m ³) | C_u (kPa) |
|--------------------|-----------------------|-------|-------------------------------|--------------------|
| Embankment | 0.2 | 0.30 | 14.7 | - |
| Crust (0-1 m) | 2.0 | 0.20 | - | 35 |
| Crust (1-2 m) | 0.8 | 0.48 | - | 25 |
| Soft clay (2-3 m) | 0.6 | 0.48 | - | 15 |
| | linear increase to | | | linear increase to |
| Soft clay (9-10 m) | 1.5 | 0.48 | - | 32 |

The undrained stiffness and in-situ stresses for the soft clay layer used in deciding on the input data for the computer calculations were those determined with the Camkometer. The undrained strengths were derived from the vane strength results. There was no data available for the stiffness of the crust and embankment material. Reasonable values were adopted for the modulus of the crust material. In the case of the embankment some preliminary F.E. calculations suggested that almost all of the material would be at or near failure, thus a rather low modulus was adopted. The soft clay was modelled as a bi-linear elastic material. Some initial F.E. calculations suggested that the soil beneath the embankment first yields when the shearing stress is about half way between the in-situ and failure values. Thus the initial modulus determined from the Camkometer results was specified for shearing stresses up to the mean of the in-situ and failure values. From this point to failure the modulus was reduced to one third of the initial value. This gives a strain at failure the same as that observed with the Camkometer. After reaching peak strength the Camkometer tests showed that the soil exhibited strain softening, but in the F.E. calculations the failure shear stress was assumed to be maintained indefinitely once the element had reached failure. The shape of the various stress-strain curves is shown in Fig. 7. The watertable was assumed to be at a depth of 1 m, hence the differing properties of the 2 layers of crust. The incompressibility of the foundation material was modelled by setting Poisson's ratio to 0.48.

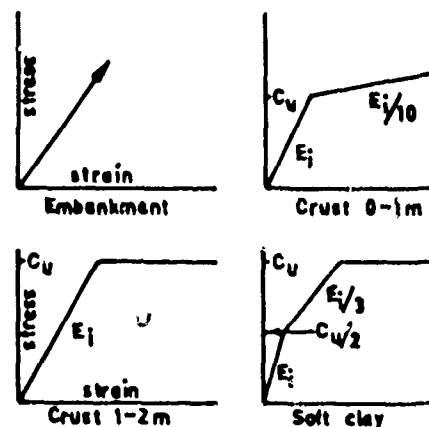


Fig. 7 Stress-strain curves for F.E. analysis

In Fig. 8 the observed undrained pore pressure response for the four piezometers under discussion is plotted against the calculated total vertical stress increase due to the embankment load at the piezometer location. Each response is seen to consist of three well defined linear portions as anticipated in section 2.

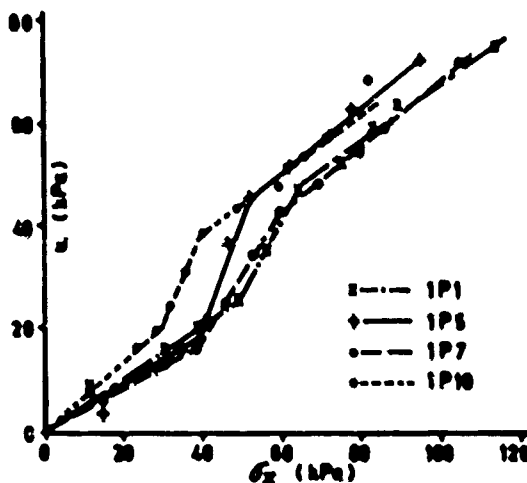


Fig. 8 Observed pore pressures against calculated vertical stress increase

In Fig. 9 the stress paths for piezometers IP1 and IP5 are plotted. The path calculated by the F.E. analysis gives total stress, the inferred effective stress path is then found by plotting the observed pore pressure values on the diagram using the total stress path as datum. Also included on the diagram for piezometer IP1 is the total stress path for a linear elastic analysis. An effective stress failure envelope for $c' = 0$ and $\phi' = 25^\circ$ is included in the diagram, these values were obtained from triaxial tests on the soil.

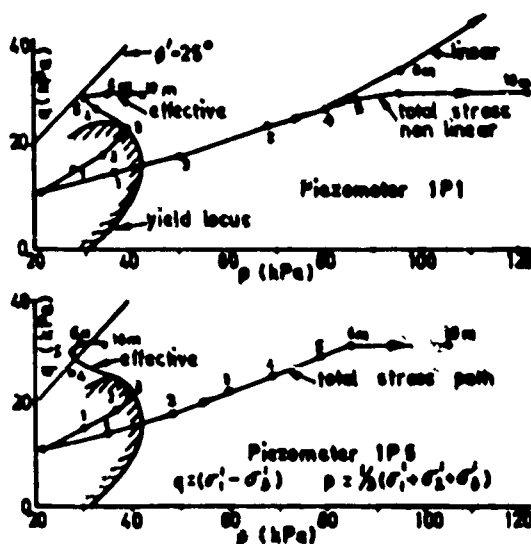


Fig. 9 Stress paths at piezometers IP1 and IP5

6 DISCUSSION

The following points merit brief comment:

(a) The finite element calculations did not attempt to eliminate any tensile stresses or to ensure that stresses in the embankment material lie within a Mohr-Coulomb failure envelope. Examination of the element stresses revealed that tensile stresses were set up in the foundation material, but these were rather smaller than the in-situ stresses. The stresses within the embankment elements were generally found to lie within a failure envelope defined by $c = 10$ kPa, $\phi = 45^\circ$, values thought to be reasonable for a compacted granular material. The major exception to this were some radial tensile stresses, up to 20 kPa, in the bottom two metres of the embankment.

(b) The yield locus was determined in triaxial stress conditions whereas the field stress conditions are more complex. A measure of the deviation of the field stress conditions from triaxial conditions is the angle, in the π plane, defined as $\tan^{-1} [(1/3)(\sigma_2 - \sigma_3)/(2\sigma_1 - \sigma_2 - \sigma_3)]$. This gives the angle between the σ_1 axis and the projection of the principal stress vector on the π plane. This angle remained fairly constant (within 3°) for a given element as the embankment height increased, and also before and after the non-linear analysis. At the location of piezometer IP1 it was -19° , at IP7 -20° and at IP10 -24° (the minus sign signifies that the angle was towards the σ_2 axis from the σ_1 axis). Thus the field stress conditions in the region of interest do not deviate much from those for triaxial compression and so the yield locus determined in the laboratory is of relevance to the field behaviour.

(c) The first kink in the pore pressure response curve, Fig. 8, corresponds approximately with the intersection of the inferred effective stress path and the yield locus, Fig. 9. Likewise for the onset of contained failure. However the initial part of the inferred effective stress path suggests that $\Delta u/\Delta \sigma_{\text{vert}}$ is 0.5 - 0.6 compared with 1.0 for an isotropic elastic soil. D'Appolonia et al (Ref. 5) and Hoeg et al (Ref. 6) found this value to be about 0.8. This difference may well be due to anisotropy in the soil and perhaps to some extent the boundary conditions in the present problem.

The rather erratic behaviour of the final part of the inferred effective stress path may be a consequence of the fact that the F.E. analysis did not consider that the soil undergoes strain softening after the peak strength. The observed pore pressure response no doubt reflects the occurrence of softening, but the F.E. stresses neglect this softening and predict rather higher values of the radial stress for the final loading stages. This could explain why the final part of the effective stress path moves away from the failure line, and also why the third stage of the pore pressure response curves in Fig. 8 does not have a slope of unity as implied in section 2.

A further aspect of this neglect of strain softening in the F.E. analysis is manifested in the decision to use the vane strengths rather than the Camkometer peak values. Some initial calculations were performed with the Camkometer strengths, but the resulting shape of the inferred effective stress paths was not satisfactory.

(d) The embankment load was applied gradually so some consolidation, with consequent changes in soil properties, must have occurred. Examination of the

amount of dissipation at the various piezometers reveals that in the soft clay layer between 2 m and 6 m pore pressures dissipated rather slowly, whereas those in the stiffer material beneath 6 m dissipated much more rapidly. Thus at day 150 (when the embankment height reached 7 m) the dissipation at piezometer IP1 was 30t and that at IP5 10t, whilst at day 120 (when 10 m was reached) the dissipations were 40t and 30t respectively. The four piezometers selected for the above comparison were located in the clay layer with the above relatively slow rate of dissipation.

(a) The effect of the non-linearity and contained failure on the computed stresses is of interest. Fig. 10a has the Mohr circles of stress at the position of IP1 when the embankment height had reached 10 m, for a linear elastic solution and that with yield and failure included. Fig. 10b has the same information at the position of IP5 with the embankment height at 7 m. It is seen that the most significant effect of the non-linear behaviour is to substantially reduce the major principal stress, σ_1 , with a rather smaller reduction in the other principal stresses.

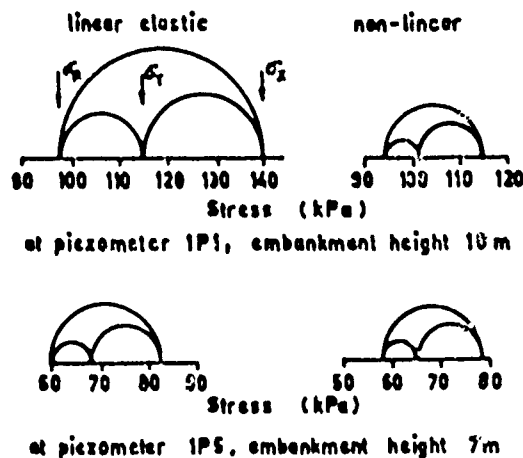


Fig. 10 Stress conditions at two piezometers

7 CONCLUSIONS

The above comparison between observed pore pressure response and calculated stress changes seems to justify qualitatively the validity of the three stage pore pressure response under field loading of lightly overconsolidated clay. The pore pressure response curves, Fig. 8, show three well defined linear portions and the inferred effective stress paths, Fig. 9, show an onset of yielding and contained failure that corresponds reasonably well with the pore pressure response.

The various aspects of the back-figuring process fit together fairly well, but qualitative conclusions only can be reached because so many features of the stress calculation are based on

drastic simplifications of the likely response of the soil. Quantitative calculations would require a more appropriate constitutive relation for the soil, in which the yield locus and plastic deformation were correctly accounted for rather than the crude bi-linear elastic model. Also the softening after peak strength and perhaps consolidation behaviour would need to be included.

8 ACKNOWLEDGMENTS

This work was done whilst the first named author was a visitor in the Engineering Department at the University of Cambridge. Financial support received from the N.Z. University Grants Committee and from a research contract funded by the U.K. Building Research Station is gratefully acknowledged.

The field measurements and much useful background information were provided by Dames and Moore, London. The field studies were commissioned by Occidental Refineries Limited.

The interest and support of Dr C.P. Wroth of Cambridge University Engineering Department is gratefully acknowledged.

9 REFERENCES

1. SCHOFFIELD, A.N. and WROTH, C.P. Critical State Soil Mechanics, McGraw-Hill, London, 1968.
2. HUGHES, J.M.O., WROTH, C.P. and PEEDER, M.J. "A Comparison of the Results of Special Pressuremeter Tests with Conventional Tests on a Deposit of Soft Clay at Canvey Island". Proc. 2nd Aust.-N.Z. Conf. on Geomechanics, Brisbane, 1975.
3. GEORGE, P.J. and PARRY, R.H.G. "Field Loading Tests at Canvey Island". Proc. Symposium: Field Instrumentation in Geotechnical Engineering, London 1973.
4. WROTH, C.P. "Pore Pressures Under Embankments", Private Communication, 1973.
5. D'APPOLONIA, D.J., LAMBE, T.W. and POULOS, H.G. "Evaluation of Pore Pressures Beneath an Embankment". Proc. ASCE Vol. 97, No. SM6, June 1971, p.881-897.
6. MOEG, K., ANDERSSON, O.B. and ROLFSEN, E.N. "Undrained Behaviour of Quick Clay Under Load Tests at Asrum". Geotechnique, Vol. 19, March 1969, p.101-115.
7. MOEG, K., CHRISTIAN, J.T. and WHITMAN, R.V. "Settlement of a Strip Load on an Elastic-Plastic Soil". Proc. ASCE, Vol. 94, SM2, March 1968, p.431-445.
8. HOLLINGSHEAD, G.W. and RAYMOND, G.P. "Prediction of Undrained Movements Caused by Embankments on Muskeg". Canadian Geotechnical Journal, Vol. 8, 1971, p.23-35.

In accordance with ER 70-2-3, paragraph 6c(1)(b), dated 15 February 1973, a facsimile catalog card in Library of Congress format is reproduced below.

Parry, R H G

Pore pressures in soft ground under surface loading; interpretation of field records, by R. H. G. Parry and C. P. Wroth, University of Cambridge, England. Vicksburg, U. S. Army Engineer Waterways Experiment Station, 1976.

1 v. (various pagings) illus. 27 cm. (U. S. Waterways Experiment Station. Contract report S-76-10)

Prepared for Office, Chief of Engineers, U. S. Army, Washington, D. C., under CWIS 31189.

Includes bibliography.

1. Clays. 2. Embankments. 3. Pore pressure.
4. Soft soils. 5. Soil deformation. I. Wroth, C. P., joint author. II. Cambridge University. III. U. S. Army. Corps of Engineers. (Series: U. S. Waterways Experiment Station, Vicksburg, Miss. Contract report S-76-10)

TA7.W34c no.S-76-10